

isardSAT®

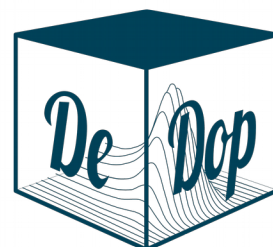
SATOC
SATELLITE
OCEANOGRAPHIC
CONSULTANTS

MSSL
UCL
Mullard Space Science Laboratory

BROCKMANN
CONSULT GMBH

Ifremer

ALONG-TRACK
.com



DeDop

Fully Adaptable and Configurable
Altimeter Delay Doppler Processor

Sentinel 3 For Science – SAR Altimetry Studies
SEOM Study 1. SARAE

DeDop Case Study Report Inland Water: Amazon river WP6400

Project reference: DeDop_ESA_TN_023

ALONG-TRACK reference: ATK_ESA_ACADDP_FR_2019_001

Issue: 0.5

Date: 2019-05-15

Activity: SEOM SARAE



Change Record

Date	Issue	Section	Page	Comment
2019-05-15	0.5	All	All	

Control Document

Process	Name	Date
Written by :	Nicolas Bercher	2019-05-17
Checked by :	Nicolas Bercher	2019-05-17
Approved by :	Nicolas Bercher	2019-05-17

Subject	DeDop Case Study <i>N</i>	Project	SARAE (DeDop)
Author	Organisation	Internal references	
Nicolas Bercher	ALONG-TRACK S.A.S.		
Pierre Fabry	ALONG-TRACK S.A.S.		

	Signature	Date
For DeDop team		
For ESA		

Contact

Institution/Company	Name
ALONG-TRACK S.A.S.	135, rue Claude Chappe ■ 29280 Plouzané ■ France Tel +33 972 655 375 ■ contact@along-track.com http://www.along-track.com/



Table of Contents

Change Record.....	2
Control Document.....	2
Contact.....	2
1 INTRODUCTION.....	5
1.1 Purpose.....	5
1.2 Document structure.....	5
1.3 Reference Documents.....	5
2 CASE STUDY DESCRIPTION.....	8
2.1 Scientific / Technical Context.....	8
2.2 Objective / Purpose of Case Study.....	10
2.3 Input Data Sets (including auxiliary and validation data sets).....	10
2.3.1 Altimetry data.....	10
2.3.2 Ancillary data.....	12
2.4 DeDop Tool Processing Specifications and Description.....	14
2.4.1 Switch from CryoSat-2 to Sentinel-3A.....	14
2.4.2 Processing Specifications.....	14
2.4.3 Processing Description.....	15
2.4.4 DeDop Test Configurations.....	17
2.5 Additional Post DeDop Processing.....	17
2.5.1 L2 Processor.....	18
2.5.2 L3 Processor.....	21
2.5.3 Validation.....	24
3 ANALYSIS OF CASE STUDY OUTPUT.....	25
3.1 Technical / Scientific Results.....	25
3.2 Impact of Different DeDop Processing Configurations.....	26
3.3 Product Validation Report.....	28
3.3.1 L3 Validation Results.....	28
3.3.2 Discussion on the L3 validation results.....	30
3.4 DeDop Processor and Tool Performance.....	31
3.4.1 DeDop Processor.....	31
3.4.2 DeDop Core Performance.....	32
3.4.3 Technical Recommendations.....	32
3.4.4 ATK's contribution to DeDop source code: ecef2lla() function.....	32
3.4.5 ATK's add-on to DeDop Core: dedop_run_scheduler.....	32
4 CONCLUSIONS / RECOMMENDATIONS.....	33
4.1 Conclusions.....	33
4.2 Recommendations.....	34
5 ACRONYMS AND DEFINITIONS.....	35
5.1 Acronyms.....	35
5.2 Definitions.....	37
5.2.1 In Altimetry.....	37
5.2.2 In Alti-Hydrology.....	37
5.2.3 In Hydrology.....	40
5.2.4 In Experimental Science.....	40
6 ANNEX A. PRESENTATION OF CASE STUDY: "INLAND WATER PROCESSING OF SENTINEL-3 L1A SARM DATA WITH DEDOP CORE".....	42
7 ANNEX B. DEDOP CONFIGURATION FILES.....	43



7.1 Configuration file #1: Basic SARM.....	43
7.2 Configuration file #2: SARM for Inland Water.....	46
8 ANNEX C. PATCH FOR DEDOP-CORE-1.5.0-LINUX-X86_64.SH INSTALLER SCRIPT	49

List of Figures

Figure 1. EIGEN-6C4+DTU13 geoid model over the South America.....	12
Figure 2. Illustration of river path data for the Amazon river.....	13
Figure 3. In situ water level data from ANA Parintins station (code 16350002).....	13
Figure 4. Block Diagram for DeDop processing steps L1A → L1B.....	16
Figure 5. Block Diagram for DeDop post-processing steps L1B → L3 and Validation.....	18
Figure 6. L2 Processor – Geoid undulations interpolated from model EIGEN-6C4+DTU13.....	19
Figure 7. L2 Processor – Ice1 retracker outputs in Sentinel-3A geophysical radargram.....	20
Figure 8. L2 Processor – Map of output Sentinel-3A L2 data with SWBD water mask.....	21
Figure 9. L3 Processor – Map of input Sentinel-3A L2 data with SWBD water mask applied.....	22
Figure 10. L3 Processor – Outputs of outliers rejection & OPO routines.....	23
Figure 11. Sentinel-3A Amazon L3 River Water Level time series with gauging data.....	26
Figure 12. Jason-2 PISTACH/Ice3 time series close to Parintins town, track 139, year 2008.....	26
Figure 13. L1B/L2 Processors – Sentinel-3A L1B geophysical radargrams with Ice1 outputs.....	28
Figure 14. Sentinel-3A Amazon Error time series of L3 Water Level.....	29
Figure 15. L3 Processor – Error evolution through the processing steps A, B and C.....	31

List of Tables

Table 1. Reference Documents.....	5
Table 2. DeDop Core – Differences between the two tested configurations.....	17
Table 3. Validation results for the L3 River Water Level time series.....	30



1 Introduction

1.1 Purpose

In this document, ALONG-TRACK S.A.S (hereafter ATK) presents the outcomes of the ACA-DDP Project, WP6400 “Inland Water Case Study”.

In this Case Study, ATK has tested configurations of the open source DeDop tool over Inland Water surfaces. Targeted application is the monitoring of river water levels based on Sentinel-3A L1A data and the run of DeDop using an appropriate delay-Doppler processing configuration.

It is important to mention that more than half of the time spent by ATK working on this case study has been done using CryoSat-2 data. However, in this report, we completely discard the work done on CryoSat-2 in order to focus on refresher results based on Sentinel-3A. Section 2.4.1 describes the motivations for the switch from CryoSat-2 to Sentinel-3A L1A data.

1.2 Document structure

This case study is about the implementation of the DeDop tool over inland water and rivers in particular. The case study document is split as follows:

- 1 Introduction
- 2 Case Study Description
- 3 Analysis of Case Study Output
- 4 Conclusions / Recommendations
- 5 Acronyms and Definitions

1.3 Reference Documents

Table 1. Reference Documents

RD-1	Birkett C.M., Mertes L.A.K., Dunne T., Costa M.H., Jasinski M.J. (2002). “Surface water dynamics in the Amazon Basin: Application of satellite altimetry”. Journal of Geophysical Research, 107 (D20), 8059, doi:10.1029/2001JD000609.
RD-2 (*)	Bercher, N. and Calmant, S. (2013c), “A review of CryoSat-2/SIRAL applications for the monitoring of river water levels”. In Living Planet Symposium (LPS2013), Edinburgh, United Kingdom. 9-13 September.
RD-3	Agência Nacional de Águas (Brazil) Web Portal : http://hidroweb.ana.gov.br/

**Table 1.** Reference Documents

RD-4	Kosuth P., Blitzkow D., Cochonneau G. (2006). "Establishment of an altimetric reference network over the Amazon basin using satellite radar altimetry (Topex/Poseidon)", in the proceedings of the "15 years of progress in radar altimetry" Symposium , Venice, Italy.
RD-5 (*)	"Précision de l'altimétrie satellitaire radar sur les cours d'eau : développement d'une méthode standard de quantification de la qualité des produits altimétriques et applications", PhD thesis (French), AgroParisTech/UMR Tétis, Montpellier, France.
RD-6 (*)	Bercher, N. and Kosuth, P. (2012a), Monitoring river water levels from space : Quality assessment of 20 years of satellite altimetry data. In Proceedings of the Symposium on "20 years of progress in radar altimetry", 24-29 September, Venice, Italy.
RD-7	SRTM Water Body Data Product Specific Guidance (v.2.0, March 12, 2003). https://dds.cr.usgs.gov/srtm/version2_1/SWBD/SWBD_Documentation/SWBD_Product_Specific_Guidance.pdf
RD-8	Förste, Ch., S.L. Bruinsma, O. Abrikosov, M. Lemoine, T. Schaller, H.-J. Götze, J. Ebbing, J.C. Marty, F. Flechtner, G. Balmino, R. Biancale, (2014). EIGEN-6C4 The latest combined global gravity field model including GOCE data up to degree and order 2190 of GFZ Potsdam and GRGS Toulouse, 5th GOCE User Workshop, Paris, 25 to 28, November, 2014. available at http://icgem.gfz-potsdam.de/ICGEM/documents/Foerste-et-al-EIGEN-6C4.pdf .
RD-9	Andersen O. .B., Knudsen P., Stenseng L. (2016). "The DTU13 MSS (Mean Sea Surface) and MDT (Mean Dynamic Topography) from 20 Years of Satellite Altimetry", Springer International Publishing, IGFS 2014", p. 111-121".
RD-10 (*)	Bercher N. with contributions from Fabry P. and Moreau T. (2017). "SAR Altimetry Processing for Inland Water: River and Lakes Monitoring". In the "SAR Altimetry Training course" of the "10th Coastal Altimetry Workshop" (CoastAlt 2017), 21-24 Feb 2017, Florence, Italy. Slides .
RD-11	Wingham D. J., Rapley C. G. and Griffiths H. "New techniques in satellite altimeter tracking systems." ESA Proceedings of the 1986 International Geoscience and Remote Sensing Symposium(IGARSS'86) on Remote Sensing: Today's Solutions for Tomorrow's Information Needs., Vol. 3. 1986.
RD-12	Ray C., Martin-Puig C., Clarizia M. P., Ruffini G., Dinardo S., Gommenginger C., Benveniste J. (2015). "SAR Altimeter Backscattered Waveform Model," in IEEE Transactions on Geoscience and Remote Sensing, vol.53, no.2, pp.911-919, doi:10.1109/TGRS.2014.2330423.
RD-13	Bercher N., Kosuth P. (2010r), " CNES R&T Study – Waveforms over Inland Water - Cemagref contribution (task 5): Validation of retracker outputs over large river of the Amazon basin ", scientific & technical report, 125 p., Dec. 3 rd 2010.
RD-14 (*)	Bercher N., Kosuth, P., Mercier, F.. (2010), "Quality and uncertainty of satellite derived river water level time series". Altimetry for Oceans and Hydrology (OST/ST meeting), 18-22 October 2010, Lisbon, Portugal. Poster.



ALONG-TRACK
.com

Project ref.: DeDop_ESA_TN_023

Issue: 0.5

Date: 2019-05-15

Page: 7 of 49

Table 1. Reference Documents

RD-15 (*)	Bercher N., Fabry P., Roca M., Martinez B., Fernandes J., Lázaro C., Gustafsson D., Arheimer B., Ambrózio A., Restano M, Benveniste J. (2016). "Validation of CryoSat-2 SAR and SARin modes over rivers for the SHAPE project". In « New era of altimetry, new challenges », Ocean Surface Topography Science Team meeting (OSTST), 31 Oct – 4 Nov 2016, La Rochelle, France. Poster.
RD-16	Laforge A., Fleury S., Guerreiro K., Birol F., Dinardo S., Sabatino G. (2018a). "Inter-comparisons of SAR processings and CryoSat-2/Sentinel-3A continuity for sea-ice observation". In Proceedings of the Symposium on "25 years of progress in radar altimetry", 24-29 September, Ponta Delgada, Azores, Portugal.

(*) Documents are available for download at <http://chronos.along-track.com/>.



2 Case Study Description

This case study is about the implementation of the DeDop tool over inland water and rivers in particular. The case study description is split as follows:

- Section 2.1 Scientific / Technical Context
- Section 2.2 Objective / Purpose of Case Study
- Section 2.3 Input Data Sets (including auxiliary and validation data sets)
- Section 2.4 DeDop Tool Processing Specifications and Description
- Section 2.5 Additional Post DeDop Processing

2.1 Scientific / Technical Context

Since the launch of ERS-1 and Topex/Poseidon, altimetry has been experimenting a lot LRM mode over inland water. Part of the issue highlighted in the processing of such data to retrieve river water levels was the large size of the LRM footprint which has been identified as potential major limitation [RD-1].

With the launch of CryoSat-2, the Alti-Hydrology community has started to experiment the new SAR and SARIN modes implemented in the SIRAL altimeter of the satellite. The high potential of the limited footprint size (in the along-track direction) offered by SAR mode has been identified as a major breakthrough [RD-2].

However, due to the increasing complexity of SAR mode compared to LRM, and the efforts required to develop in-house delay-Doppler processors, working with SARM data remained a complicated task. The technique was new to the altimetry community and, as expertise ramped up quickly, the tools were being developed accordingly. This resulted in a wide variety of configuration options to be tested with delay-Doppler processors and associated datasets to be analysed. In Alti-Hydrology, this situation has been entangled with the sparse and changing availability of CryoSat-2 data around the globe (about 16% covered in SARM and 16% in SARINM) with few masks actually implemented over inland water (parts of the Amazon basin and a few rivers: Mekong, Congo, Danube, Brahmaputra, Ganges, etc.).

The community quickly identified the lack of some key variables into CryoSat-2 data products. Actually, the available products (Baselines A, B and C) from the CryoSat-2 ground segment processor were: FBR (=L1A), L1B and L2 [RD-2]. However, SARM relies on the construct of Stack matrices¹, used to compute the SAR waveforms priori retracking. And not having Stack matrices in data products (now available in Sentinel-3 products catalogue under the "L1BS" denomination) has been an important lack for Alti-Hydrology. Actually, Stack matrices offers the opportunity to develop on the shoulders of several innovative approaches:

- The use of the Range Integrated Power (RIP): sum of the Stack matrix along the range dimension, from which statistical parameters can be derived to provide information on the specular characteristics of the observed reflectors.

¹ Stack matrices are series of delay-Doppler radar echoes (aka, Doppler beams), computed as estimation of radar echoes coming from the same surface on the ground but from different view angles, as the satellite moves forward along its trajectory.



- The use of the Stack itself, including:
 - For decontamination purposes: because of the “side-lobe”² effect, “ghosting echoes” can occur in presence of highly specular surfaces seen from particular looking angles. Thus, some of the Doppler beams of the Stack can be contaminated by such effect,
 - For the test of alternate “waveform stacking” (averaging) strategies, e.g., known as Stack Masking.
 - For signal improvement and gain compensation, e.g., AC/DC developed by Chris Ray and isardSAT [RD-12].
 - For Waveforms modelling, e.g., taking into account for surface roughness, to estimate the radar echoes peakiness and improve the fitting of the waveforms by models.

These approaches are of high interest for applications over inland water, but also for other surfaces such as the sea ice. ESA R&D projects dealing with these topics are numerous (e.g., CRUCIAL, SHAPE, ACA-DDP, Cryo-seaNice).

Before the development of DeDop, only a few SARM (and SARINM) processors were producing data: basically, the ESA CryoSat-2 IPF1 processor (SARM, SARINM), CNES CPP (SARM only) and GPOD/SARVatore (initially SARM, then SARINM a few years later with SARINVatore).

Apart from the official ESA IPF processor, CNES CPP (dedicated to SARM only) has been used by French teams (CNES, CLS, LEGOS) and tested on inland water but for fixed, thus limited, processing configurations. On the other hand, the GPOD/SARVatore has been made available as an online tool and since allows to batch processing runs, parametrised by user’s configurations (a breakthrough!). The tool has soon offered new options, in particular the ability to output Stack matrices as part of L1BS products files, extending the traditional L1B files.

Nonetheless, few drawbacks are inherent to GPOD/SARVatore:

- It is only available to be run remotely, from online servers, and can’t be automated nor integrated with other tools.
- Despite its versatile evolution and the very nice synergy of the development team with their users, it is a tool that can’t be pushed further. Notably if comes the need for high level users (e.g, engineers, researchers) to be modified, extended or even debugged, etc.

DeDop, being open source and having a (simple and) automatable interface (DeDop core), it solves the drawback of GPOD/Salvatore mentioned above. Feedback examples from this Case Study are provided in section 3.4.4 and section 3.4.5.

Related references:

- [RD-10] – “SAR Altimetry Training course on SAR” of the 10th Coastal Altimetry Workshop, CoastAlt 2017, by Bercher et al. (ATK).

² The side-lobes of the antenna spatial gain pattern.



2.2 Objective / Purpose of Case Study

The general objectives of the study are to demonstrate:

- The usability of the DeDop tool.
- The adequacy of the DeDop tool for the purpose of monitoring river water levels.
- The performances of the DeDop tool.
- The benefits of a configurable delay-Doppler processor.
- The benefits of the free access to the source code of the DeDop tool.

Regarding Inland Water, the main objective is to quantify the benefit of the ability to customize a the configuration of the delay-Doppler processor (versus a basic configuration).

These objectives are conditioned by secondary objectives:

- To produce Stack matrices data and examine them.
- To produce Waveforms and examine them.
- To elaborate a look-a-like L2 data for the L3 processor, despite the absence of L2 atmospheric a geophysical corrections (the geoid being a critical one) and retracking algorithm in the DeDop suite.
- To produce a L3 data: River Water Level (RWL) time series.
- To perform validation of the L3 RWL data against in situ gauging data.
- To analyse and comment results, provide recommendations, etc.

2.3 Input Data Sets (including auxiliary and validation data sets)

2.3.1 Altimetry data

The Case Study uses Sentinel-3A L1A data as input for the DeDop processor. The L1A products files have been downloaded from the scihub portal³, then edited in order to remove useless data records outside latitude boundaries.

2.3.1.1 Space & Time Constraints

In order to perform real validation activity, some constraints has been applied to match the space & time availability of gauging data. The result of this assessment in summarised in the list below:

- **Space**
 - **Geo Bouding Box:** ($\text{lat} \in [-5.0^\circ; -2.0^\circ]$) \cap ($\text{lon} \in [-57.8; -55.8]$)

3 <https://scihub.copernicus.eu/dhus/>



- **Sentinel-3A Track:** 316
- Note: Track 316 is the closest to gauging station over the Amazon river.
- **Time**
 - **Time period:** from 2016-06-24 to 2018-10-09
 - **Sentinel-3A Cycles:** from 005 to 036
 - Note: Gauging data are made available after some delay ranging from 1 to 12 months depending on the station/subbasin.

The resulting list of L1A product files intersecting these space-time constraints is:

S3A_SR_1_SRA_A_20160624T012403_20160624T021432_20170624T145714_3029_005_316_____MR1_R_NT_002.nc
S3A_SR_1_SRA_A_20160721T012401_20160721T021430_20170625T012402_3029_006_316_____MR1_R_NT_002.nc
S3A_SR_1_SRA_A_20160817T012401_20160817T021430_20170625T135354_3029_007_316_____MR1_R_NT_002.nc
S3A_SR_1_SRA_A_20160913T012403_20160913T021432_20170626T062023_3029_008_316_____MR1_R_NT_002.nc
S3A_SR_1_SRA_A_20161010T012405_20161010T021434_20170626T165014_3029_009_316_____MR1_R_NT_002.nc
S3A_SR_1_SRA_A_20161106T012402_20161106T021431_20170627T024110_3029_010_316_____MR1_R_NT_002.nc
S3A_SR_1_SRA_A_20161203T012400_20161203T021428_20170627T121502_3028_011_316_____MR1_R_NT_002.nc
S3A_SR_1_SRA_A_20161230T012402_20161230T021430_20170627T214854_3028_012_316_____MR1_R_NT_002.nc
S3A_SR_1_SRA_A_20170126T012403_20170126T021432_20170628T072158_3029_013_316_____MR1_R_NT_002.nc
S3A_SR_1_SRA_A_20170222T012401_20170222T021430_20170629T013326_3029_014_316_____MR1_R_NT_002.nc
S3A_SR_1_SRA_A_20170321T012402_20170321T021431_20170629T101703_3029_015_316_____MR1_R_NT_002.nc
S3A_SR_1_SRA_A_20170417T012406_20170417T021436_20170512T201053_3029_016_316_____LN3_O_NT_002.nc
S3A_SR_1_SRA_A_20170514T012406_20170514T021436_20170608T201150_3029_017_316_____LN3_O_NT_002.nc
S3A_SR_1_SRA_A_20170610T012406_20170610T021436_20170705T201126_3029_018_316_____LN3_O_NT_002.nc
S3A_SR_1_SRA_A_20170707T012406_20170707T020807_20170801T235417_2640_019_316_____LN3_O_NT_002.nc
S3A_SR_1_SRA_A_20170707T012406_20170707T021436_20170801T233843_3029_019_316_____LN3_O_NT_002.nc
S3A_SR_1_SRA_A_20170707T012406_20170707T021436_20170801T235731_3029_019_316_____LN3_O_NT_002.nc
S3A_SR_1_SRA_A_20170803T012406_20170803T021436_20170828T214911_3029_020_316_____LN3_O_NT_002.nc
S3A_SR_1_SRA_A_20170830T012407_20170830T021436_20170925T013126_3029_021_316_____LN3_O_NT_002.nc
S3A_SR_1_SRA_A_20170926T012406_20170926T021436_20171021T211121_3029_022_316_____LN3_O_NT_002.nc
S3A_SR_1_SRA_A_20171023T012407_20171023T021436_20171118T002027_3029_023_316_____LN3_O_NT_002.nc
S3A_SR_1_SRA_A_20171119T012407_20171119T021436_20171214T214421_3029_024_316_____LN3_O_NT_003.nc
S3A_SR_1_SRA_A_20171119T012407_20171119T021436_20171215T130126_3029_024_316_____LN3_O_NT_003.nc
S3A_SR_1_SRA_A_20171216T012407_20171216T021436_20180111T012049_3029_025_316_____LN3_O_NT_003.nc
S3A_SR_1_SRA_A_20180112T012407_20180112T021436_20180207T011146_3029_026_316_____LN3_O_NT_003.nc
S3A_SR_1_SRA_A_20180208T012407_20180208T021436_20180305T225716_3029_027_316_____LN3_O_NT_003.nc
S3A_SR_1_SRA_A_20180307T012410_20180307T021439_20180401T225121_3029_028_316_____LN3_O_NT_003.nc
S3A_SR_1_SRA_A_20180403T012412_20180403T021441_20180428T213803_3029_029_316_____LN3_O_NT_003.nc
S3A_SR_1_SRA_A_20180430T012415_20180430T021444_20180525T214003_3029_030_316_____LN3_O_NT_003.nc
S3A_SR_1_SRA_A_20180527T012414_20180527T021444_20180621T225353_3029_031_316_____LN3_O_NT_003.nc
S3A_SR_1_SRA_A_20180623T012416_20180623T021445_20180718T213706_3029_032_316_____LN3_O_NT_003.nc
S3A_SR_1_SRA_A_20180720T012414_20180720T021443_20180814T213640_3029_033_316_____LN3_O_NT_003.nc
S3A_SR_1_SRA_A_20180816T012411_20180816T021440_20180910T213523_3029_034_316_____LN3_O_NT_003.nc
S3A_SR_1_SRA_A_20180912T012412_20180912T021441_20181008T002603_3029_035_316_____LN3_O_NT_003.nc
S3A_SR_1_SRA_A_20181009T012415_20181009T021444_20181103T210604_3029_036_316_____LN3_O_NT_003.nc

IMPORTANT: The files listed in **red** are duplicate cycle/track pass files that overlap each other for **all** or **parts** of their data records. **This is a bug in scihub system and/or in the Sentinel-3A ground segment.**

ATK has discarded files which are shorter in terms of covered time interval and/or which are older in terms of processing date:

Cycle 019 / Track 316:

S3A_SR_1_SRA_A_20170707T012406_20170707T020807_20170801T235417_2640_019_316_____LN3_O_NT_002.nc
S3A_SR_1_SRA_A_20170707T012406_20170707T021436_20170801T233843_3029_019_316_____LN3_O_NT_002.nc

Cycle 024 / Track 316:

S3A_SR_1_SRA_A_20171119T012407_20171119T021436_20171214T214421_3029_024_316_____LN3_O_NT_003.nc



2.3.2 Ancillary data

Some ancillary data necessary in this Case Study have been provisioned and setup in order to fulfilled the needs of the L2 and L3 Processors as well as those of the Validation tools.

2.3.2.1 L2 Processor

In order to build L2 data, some ancillary data have been provisioned and added to DeDop Core L1B data:

- **Geoid:** EIGEN-6C4+DTU13

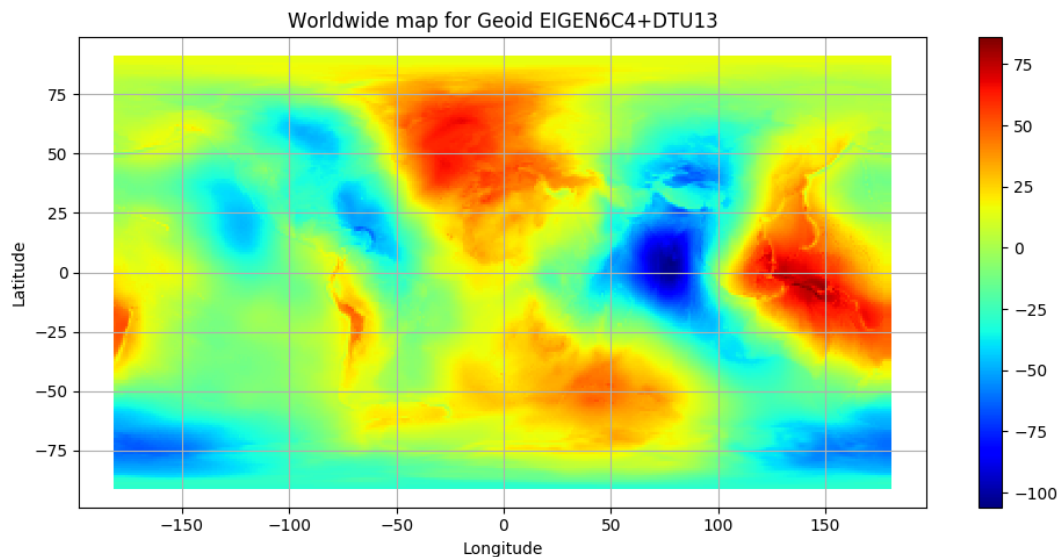


Figure 1. EIGEN-6C4+DTU13 geoid model over the South America

- **L2 Atmospheric Corrections:** Derived from Jason-3, same place, same time.

2.3.2.2 L3 Processor

- Water Mask data: SWBD [RD-7] & Edited SWBD (restrict to the studied ROI), cf. Fig. 8

The SWBD water mask is used for representation purposes only while the SWBD-Edited water mask is used for computational purposes, in order to isolate water surface altimetry records from the others. (SWBD-Edited is an internal dataset produced by LEGOS and ATK.)

- River path data

The river path data is a geolocated linestring feature (red curve in Fig. 2) that follows the central line of the river path. It can be made manually (in this case) or automatically derived from water mask data. This data is used to compute the curvilinear distance (from river mouth) to be associated to Altimetry measurements.



Typically, this distance is used to represent data against the longitudinal graphs and perform other computations in the L3 Processor.

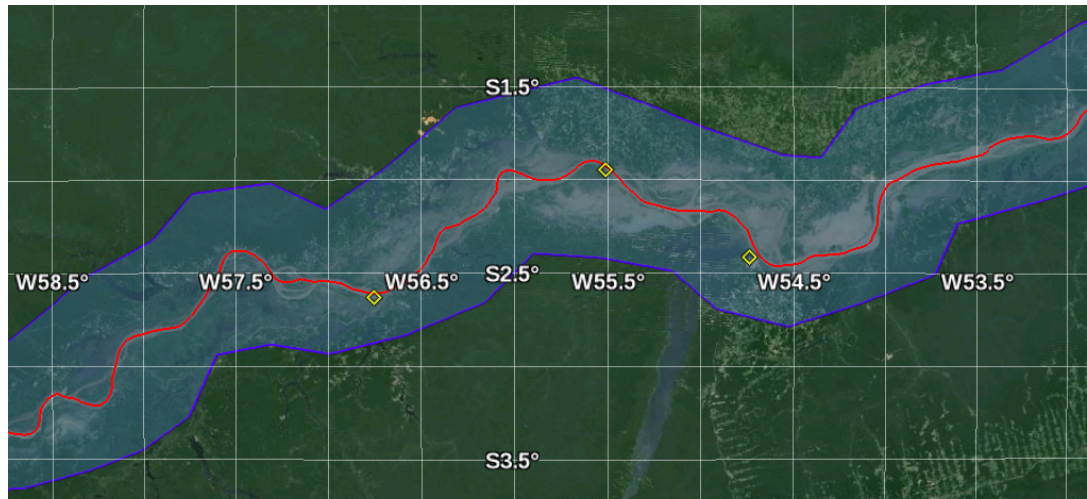


Figure 2. Illustration of river path data for the Amazon river
The river path is a geolocated linestring (red curve) that describes the central line of the river.

2.3.2.3 Validation: In situ Gauging data

Gauging station in situ water level: ANA data from Parintins station, code 16350002, cf. Fig. 3. Original water level data from ANA database are provided as relative water level variations. The spirit levelling of the data has been done using levelling informations from Kosuth et al. (2006) [RD-4].

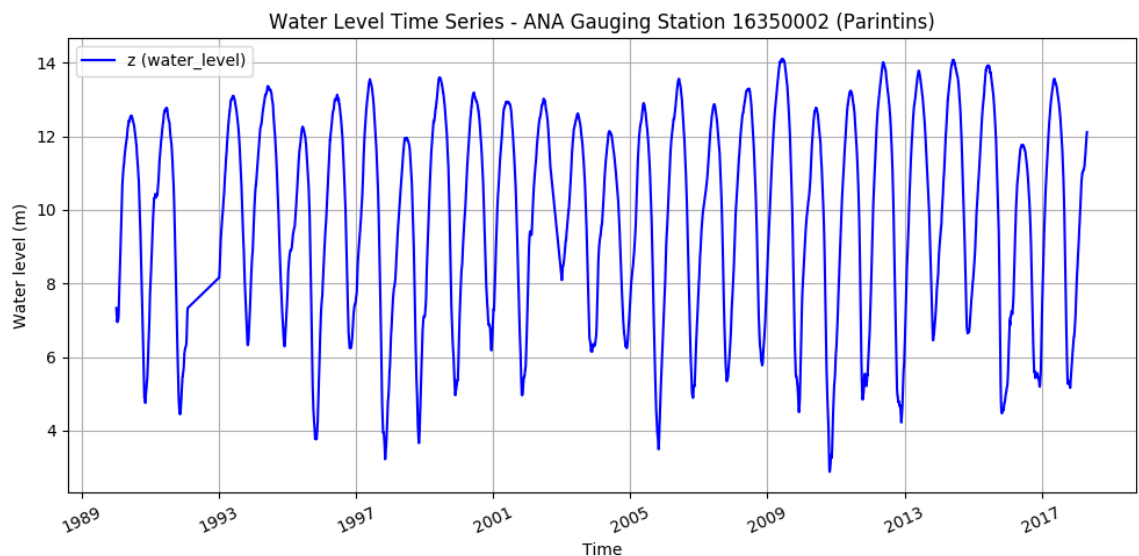


Figure 3. In situ water level data from ANA Parintins station (code [16350002](#))



2.4 DeDop Tool Processing Specifications and Description

The DeDop Core tool, part of the DeDop tools, is the only component implemented in this Case Study. In this section, we report on the processing specifications & description, as well as the configurations of the delay-Doppler DeDop Core that has been implemented and tested.

2.4.1 Switch from CryoSat-2 to Sentinel-3A

Initially, this Case Study was setup to work with CryoSat-2 SARM data as input to the DeDop tool. This was because at the time of proposal/KO, Sentinel-3A was not launched yet. However, with time passing, the team decided to switch to real Sentinel-3A L1A data.

The main elements of motivation for the switch were:

1. **ACA-DDP Project is “Sentinel-3A oriented”**: having such data available during the course of the project not initially guaranteed, but after months after the launch of Sentinel-3A using the switch became an obvious option.
2. **Overhead in converting CryoSat-2 L1A files to the format of Sentinel-3A**: actually ATK obtained and processed CryoSat-2 L1A data files (~230 files, 72GB) and processed them using DeDop Core versions 1.0.0, 1.1.0, 1.2.0, 1.3.0 and 1.4.0. However, after lots of investigations and corrective operations, the overall quality of the data at L2 stage was not judged as satisfactory.
3. **CryoSat-2 has a geodesic orbit**: this would have made the L3 processing steps more complex which is not the intent of this case study.

2.4.2 Processing Specifications

2.4.2.1 DeDop Core version & system compatibility

The DeDop Core version that has been used for this Case Study is the Linux 64 bit [DeDop-core-1.5.0-Linux-x86_64.sh](#) bundle release in version 1.5.0. This package-script embeds all-in-one, autonomous, set of complete libraries needed to run DeDop Core. Despite being disk space consuming (~1.5GB), these DeDop releases are very convenient to end users since they can be installed anywhere on the target machine and **without any particular adaptation nor undesired interactions** with the hosting operating system environment. The only requirements rely on the compatibility of the DeDop bundle libraries with the Linux system calls on the target machine. Linux API being fairly stable in time, this approach is considered very perennial.

ATK has easily deployed and tested several versions of DeDop Core before v1.5.0 on several machines: v1.0.0, v1.1.0, v1.2.0, v1.3.0, v1.4.0 and finally v1.5.0.



2.4.2.2 Need for parallel runs of DeDop Core

DeDop Core exhibits fairly good computational performances. However, it is not able to process L1A files in parallel which is unfortunate since nowadays machines all have, at least, dual logical core CPUs. In order to improve computational time, ATK used [dedop_run_scheduler](#) script (as described in section 3.4.5).

The combination of DeDop Core and the [dedop_run_scheduler](#) allowed ATK to run DeDop on CPU servers as well as on high-grade laptop machines which turned to be very convenient.

We report below on some typical ATK's machines specification and the improvement induced by the use of the [dedop_run_scheduler](#) tool on them:

CPU server specifications (since 2019)

- Intel Xeon Silver 4110, 32 logical cores, 144GB DDR4 RAM, RAID6 storage
- Computation time:
 - With [dedop_run_scheduler](#): 90 seconds (x32 faster)
 - DeDop Core alone: 48 minutes

Laptops specifications (since 2017)

- Intel Core i7 7th generation, 4 logical cores, 16GB DDR4 RAM, SSD storage
- Computation time:
 - With [dedop_run_scheduler](#): 18 minutes (x4 faster)
 - DeDop Core alone: 72 minutes

2.4.3 Processing Description

This section presents description of the processing done with the DeDop Core tool. The processing steps which are described below have been applied identically to the L1B data outputted by DeDop for the two tested configurations.

Fig. 4 provides an overview of the L1A to L1B processing steps.

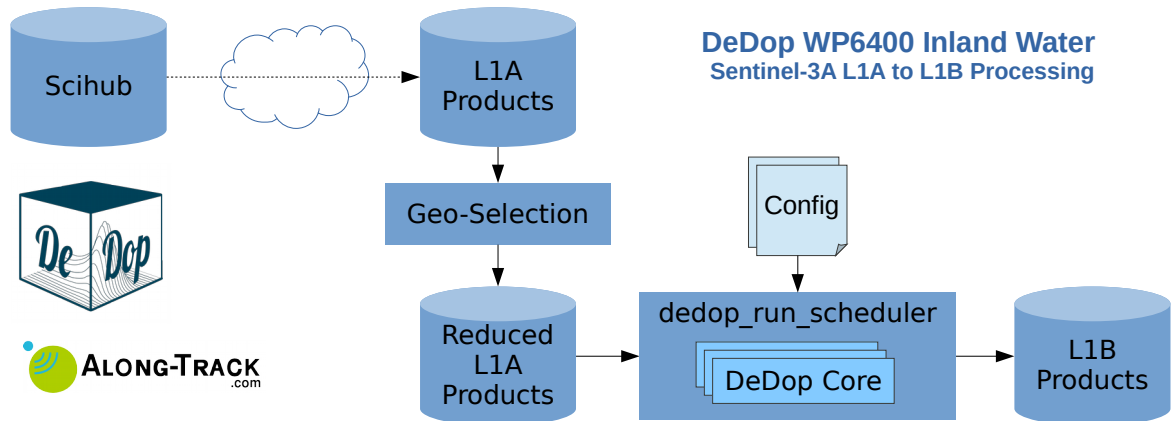


Figure 4. Block Diagram for DeDop processing steps L1A → L1B

2.4.3.1 Geo-selection of L1A data records

The Sentinel-3A L1A files downloaded from the SciHub portal contain along-track pole-to-pole data records.

Before running DeDop, the Sentinel-3A L1A files have **been truncated** in order to remove data records outside of the latitude interval around the Amazon river. This was necessary to reduce the overall computational time of all of the L1A files. The truncation has been done based on latitude values to centre data around the ROI (Amazon river, Parintins town), for interval `lat < [-5.0 ; -2.0]`, which largely embrace the records required to properly build Stack data long before the crossing over the river.

The resulting files have been set `.parintins.nc` file extension, **they are the L1A input files for this Case Study**, e.g., for the first source L1A file:

`S3A_SR_1_SRA_A_20160624T012403_20160624T021432_20170624T145714_3029_005_316_____MR1_R_NT_002.parintins.nc`

The overall size of L1A files to be processed after files truncation is 2.41 GB.

2.4.3.2 Production of L1B files

ATK has been running DeDop Core for the two configurations described in section 2.4.4. As illustrated in Fig. 4, the runs of DeDop Core have been done with the `dedop_run_scheduler` script. The outputs are L1BS (not used in this Case Study) and L1B product files corresponding to all of the input L1A files.

It is worth mentioning that after all optimisations implemented by ATK (`ecef2lla()` routine, job scheduler and L1A files truncation), the production of the L1BS+L1B files takes about 90 seconds on ATK's CPU server (cf. section 2.4.2.2).



2.4.3.3 Failures of the DeDop Core and Installer

Early versions of DeDop Core implemented an iterative algorithm for the computation of geographical coordinates, from ECEF custom ellipsoid model. A patch including an alternate implementation of the routine has been used by ATK to solve this issue. The related patch has since been integrated in the DeDop Core codebase, cf. Section 3.4.4, solving Issue#31 on GitHub.

Due to an error in self-sanity checking of the installation script, ATK had to patch file [DeDop-core-1.5.0-Linux-x86_64.sh](#) for it to install properly (cf. patch provided in Annex C). This issue and patch have been reported to the developers team. It is worth noting that this issue is apparently due to some regression affecting the installer releases since v1.4.0.

2.4.4 DeDop Test Configurations

The DeDop Core tool has been run for two different configurations:

1. Configuration #1: Dedicated to do basic SARM processing
2. Configuration #2: Dedicated to do optimised SARM for Inland Water

The differences between the two configurations are listed in Table 2 below:

Table 2. DeDop Core – Differences between the two tested configurations

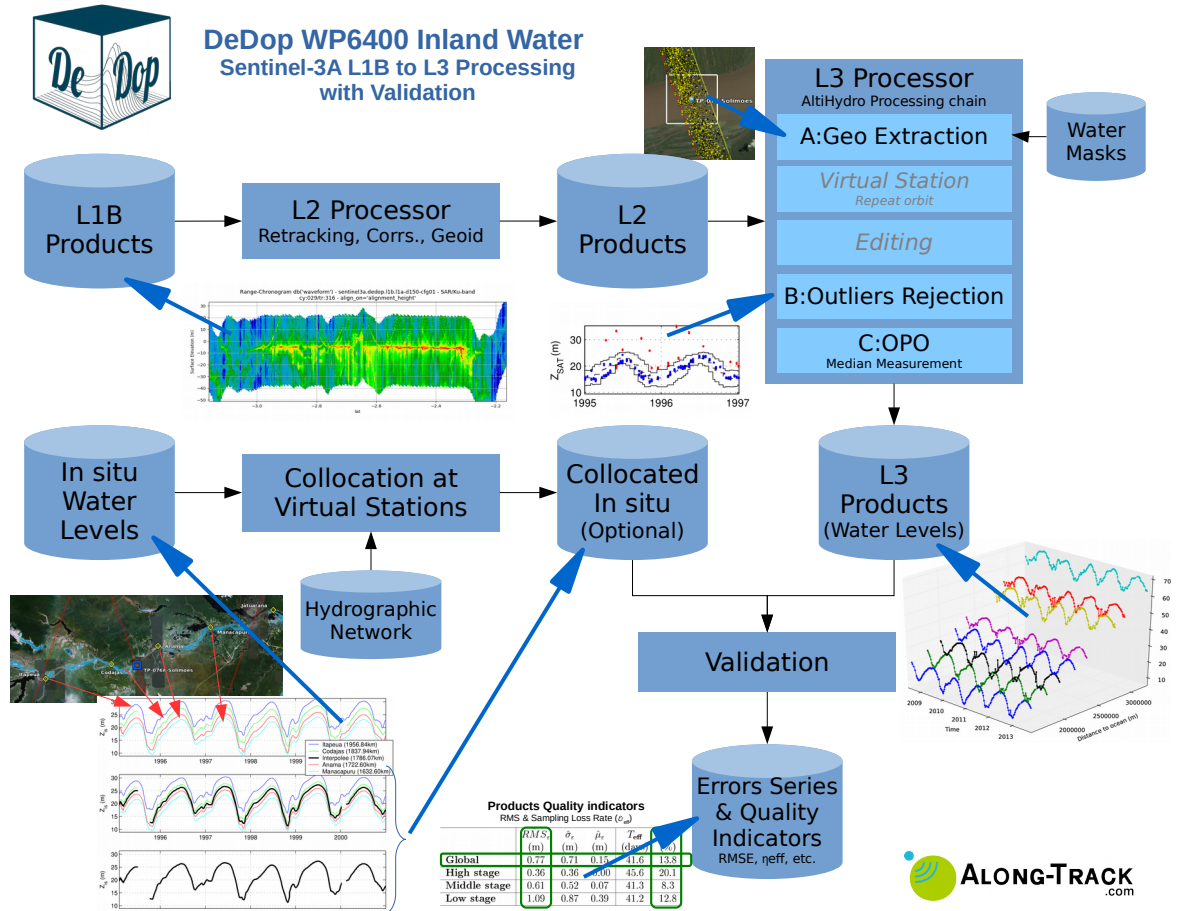
Parameter	Conf. #1: Basic	Conf. #2: Inland Water
Azimuth Windowing	None	Hamming
Azimuth Processing Method	Approx	Exact
Zero Padding Factor	1	2

The Complete configuration files (CNF.json) for the two configurations are provided in Annex B.

2.5 Additional Post DeDop Processing

This section introduces to the additional Processors that have been necessary prior to the validation of Altimetry data over rivers. The processing steps which are described below have been applied identically to the L1B data outputted by DeDop for the two tested configurations.

The following subsections provide details on the processing steps, and illustrations for some of intermediate key results, of the L2 & L3 processors and the validation tools. Fig. 5 provides an overview of these additional processing & validation steps.



2.5.1 L2 Processor

The main steps of the L2 Processor implemented for this case study are:

1. Read input netCDF L1B data files, cf. data map in Fig. 8
2. Compute **Waveforms alignment** w.r.t. the onboard tracker taking account for L2 corrections, geoid exclude (e.g., used to plot geophysically significant radargram graphics like in Fig. 7)
3. Compute **Geoid undulation**, cf. Fig. 6
4. Run **Ice1 retracker** on Waveforms, cf. radargram in Fig. 7
5. Compute water masking against SWBD (for the purpose of radargram plots like in Fig. 7)



2.5.1.1 Geoid – EIGEN-6C4+DTU13

Fig. 6 below represents the undulation (in metres) of the Geoid EIGEN-6C4+DTU13 [RD-8] [RD-9], as a function of latitude (in decimal degrees).

Due to the large variations of the Earth gravity field, the geoid undulation values are essential to inland water studies. The amplitude of the undulations are about 6 metres along the Sentinel-3A track 316.

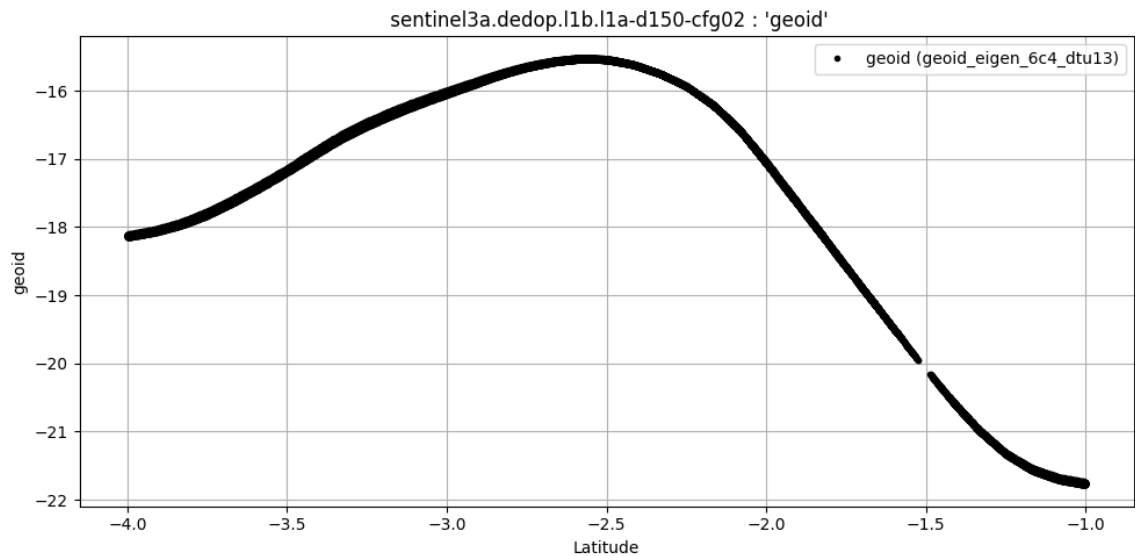


Figure 6. L2 Processor – Geoid undulations interpolated from model EIGEN-6C4+DTU13. Geoid values (in metres) along the repeated passes of Sentinel-3A on track 316 (coordinates from DeDop’s L1B data records).

2.5.1.2 Ice1 retracker

The Ice1 retracker implemented in this study, codename “Ice1g”, is a generalised and very fast Python implementation (owned by ATK) of the traditional Ice1 retracker [RD-11]. It can optionally retrack several peaks at once from within the same waveform. For this study, the number of retracked peaks per waveform has been set to 1 in order to obtain, process and study usual outputs (i.e., one record → one range value). This implementation is able to retrack about 100 000 waveform echoes per second on standard laptops.

Figure 7 below illustrates outputs of the Ice1 retracker on top of L1B Sentinel-3A waveforms radargram. For this case study, **Ice1 threshold value has been set to 0.87**. This value is commonly used for SARM waveforms which are do not follow the same progression in time compared to LRM waveforms (for which a threshold value of 0.3 is usually applied).

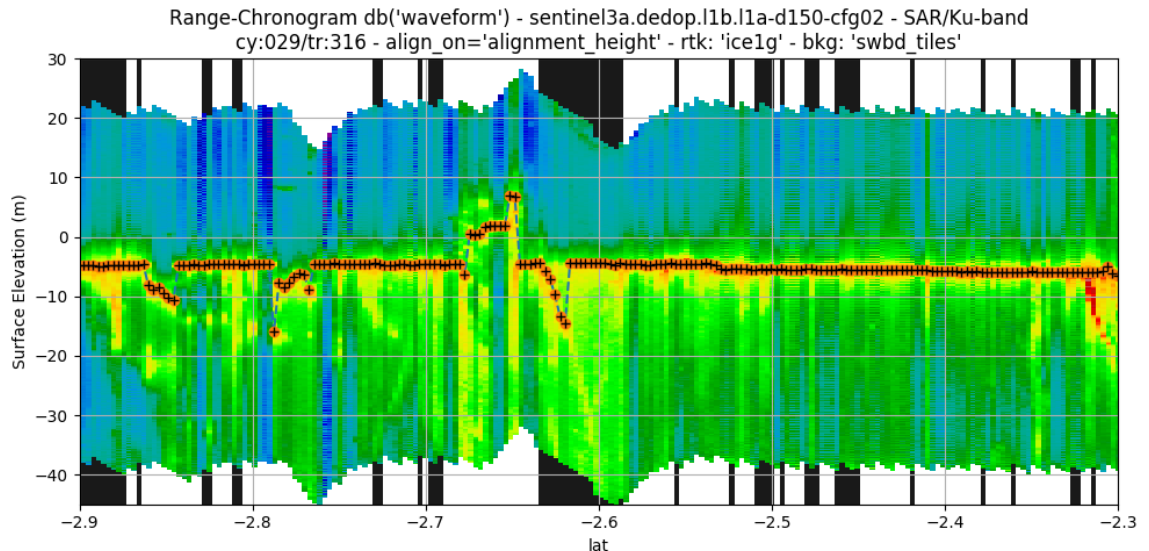


Figure 7. L2 Processor – Ice1 retractor outputs in Sentinel-3A geophysical radargram. L1B data from DeDop’s configuration#2, cycle 29/track 316 over the Amazon river. Ice1 outputs are black ‘+’ in orange dots. Vertical black patches in the background mark altimetry records acquired into the SWBD water mask.

2.5.1.3 Output Sentinel-3A L2 data map (with auxiliary data)

Figure 8 below is the map of the inland Water Case Study over the Amazon river near Parintins town. It represents:

- **Background light grey:** Polygons of the SWBD water mask, used for illustration purposes only
- **Background blue:** Polygons of the SWBD-Edited water mask (isolates the main river channel), used for processing purposes (L3)
- **Scatter plot / coloured dots:** Location and surface height (noted ‘**z**’) derived from Sentinel-3A altimetry L2 data (=upgraded L1B with retracking, corrections and geoid)
- **Black/yellow circle:** Location of the gauging station of Parintins town

In this case study, the gauging data and the crossing between satellite tracks and the river are very close. This avoids additional steps usually necessary to do data collocation prior validation.

For a zoom around the river crossing the reader is invited to look at Fig. 9.

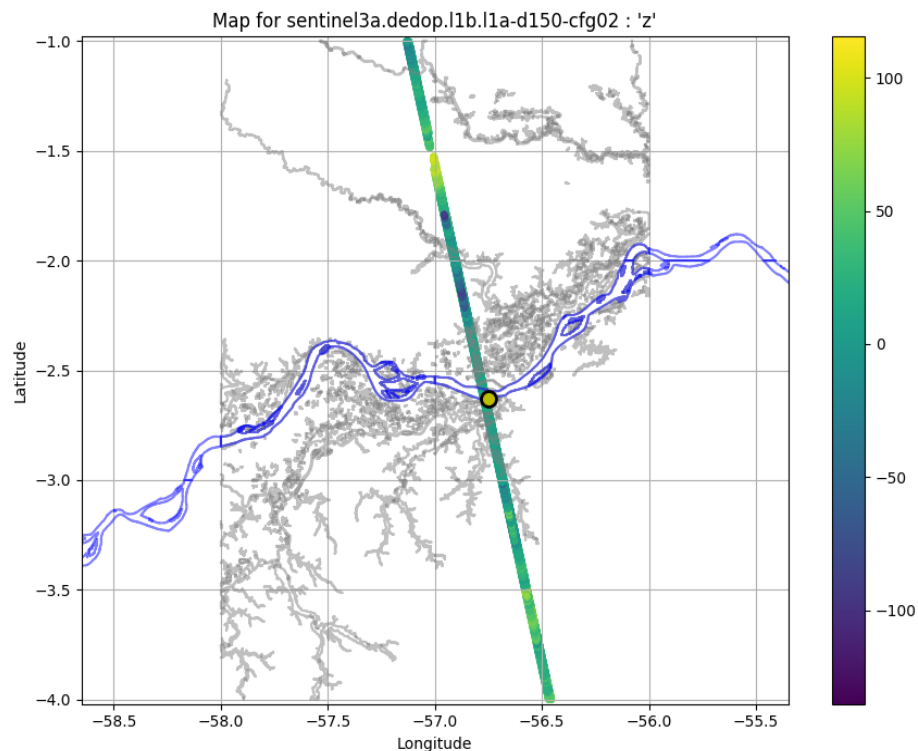


Figure 8. L2 Processor – Map of output Sentinel-3A L2 data with SWBD water mask
Scatter plot of surface height from L2 data (includes geoid), background: SWBD water mask (grey) and SWBD-Edited (blue) ; Location of the Parintins gauging station (black/yellow circle).

2.5.2 L3 Processor

The main steps of the L3 Processor implemented for this case study are:

1. Compute **water masking** against SWBD-Edited (boolean flag variable), cf data map in Fig. 9
2. Compute **surface height** variable based on Ice1 range values and corrections, cf Fig. 10 (top):
 - **Geoid** undulations (EIGEN-6C4+DTU13)
 - **Static range corrections** (estimated from Jason-3 GDR-d data, same place, same time)
3. Run **outlier rejection** routines, cf. Fig.10 (top middle plot):
4. Run **OPO** routines (in order to get “One (measurement) Per Overflight”), cf. Fig.10 (bottom middle plot)

2.5.2.1 Water masking

Figure 9 below is the map of the L2 data after water masking (L3 processor’s step 1) to be used to produce L3 RWL time series over the Amazon river near Parintins town. It represents:



- Background light grey: Polygons of the SWBD water mask
- **Background blue**: Polygons of the SWBD-Edited water mask (isolates the main river channel)
- Scatter plot / coloured dots: Location and surface height (noted 'z') derived from Sentinel-3A altimetry L2 data
- Black/yellow circle: Location of the gauging station of Parintins town

In this case study, the gauging data and the crossing between satellite tracks and the river are very close. This avoids additional steps usually necessary to do data collocation prior validation.

For a zoom around the river crossing the reader is invited to look at Fig. 8.

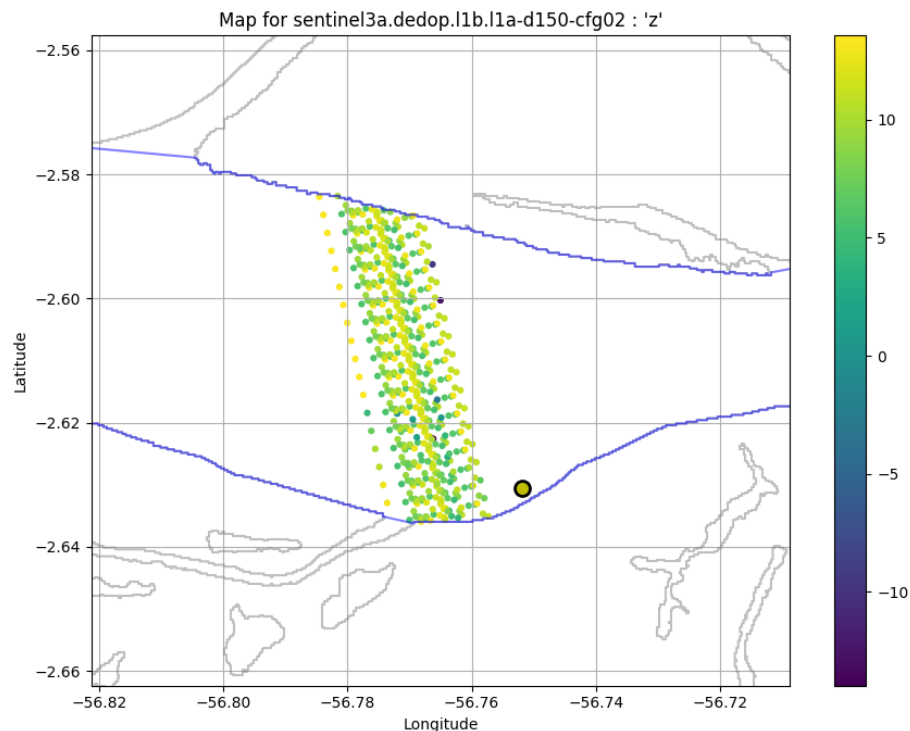


Figure 9. L3 Processor – Map of input Sentinel-3A L2 data with SWBD water mask applied. Scatter plot of surface height from L2 data (includes geoid), background: SWBD water mask (grey) and SWBD-Edited (blue). Location of the Parintins gauging station (black/yellow circle).



2.5.2.2 Outliers rejection and OPO

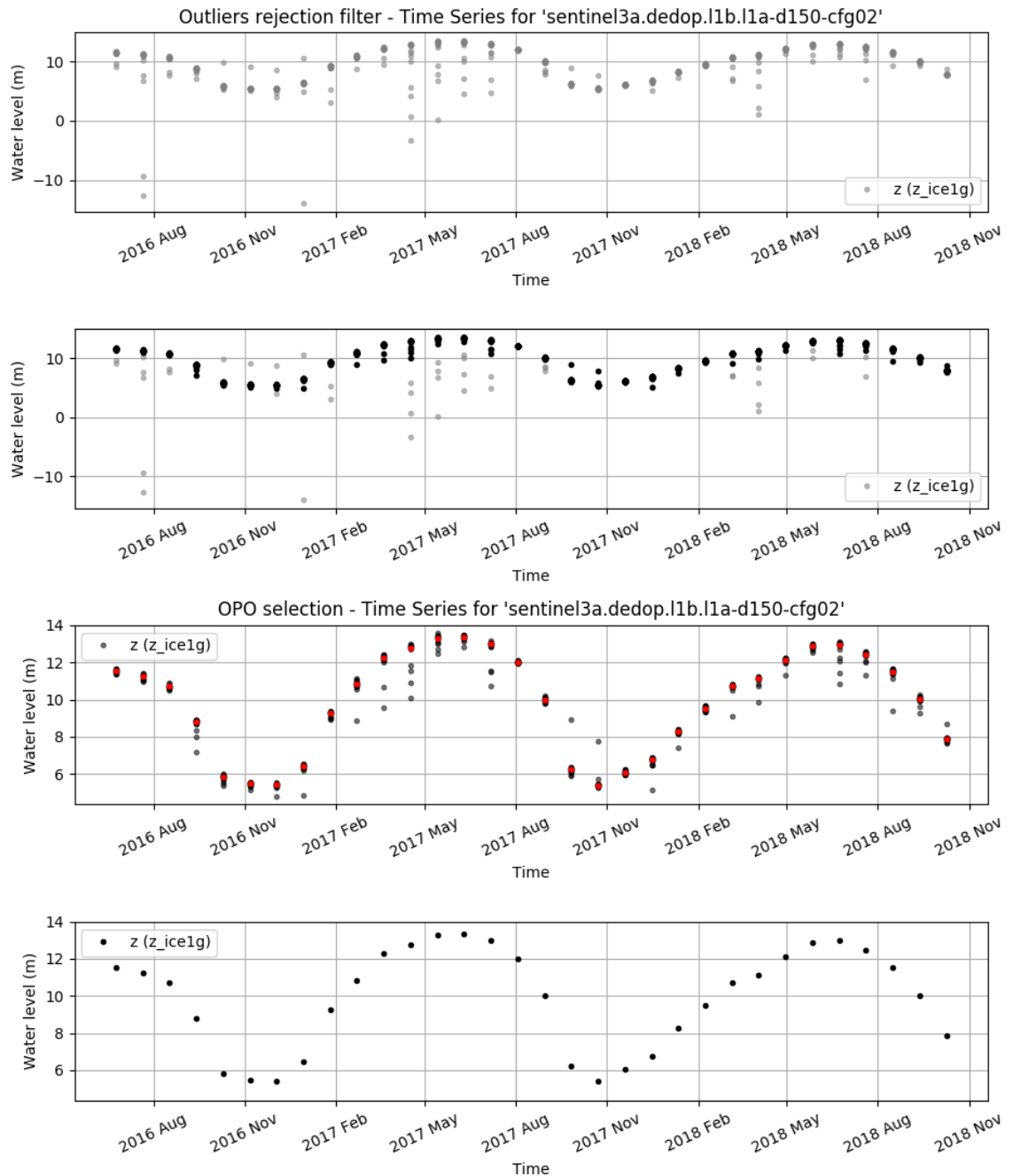


Figure 10. L3 Processor – Outputs of outliers rejection & OPO routines

(Top) Step A: L2 data selected from within the water mask. (Middle's top) Step B: Result of outliers rejection filters (black dots) among all L2 data (grey dots). (Middle's bottom) Step C: Result of OPO routine (red dots) among filtered L2 data (black dots). (Bottom) Final L3 River Water Level time series (=outputs of Step C only).



2.5.3 Validation

The validation methodology implemented in this activity has been used on numerous LRM missions [RD-6] (ESA 20YPRA symposium presentation) and extensively described in [RD-5] (Bercher, French PhD thesis, 2008).

The main steps of the validation implemented for this case study are:

1. Prepare L3 data:
 - **Collocation:** *This step is useless in this case since data are naturally collocated in space*
 - **Codation:** Restrict data to common time interval and time stamps
2. Read in situ gauging data from ANA database, for Parintins gauging station (code 16350002), cf. Fig. 3
3. Run validation tools:
 1. Compute **error time series** of the water level measurements
 2. Compute **quality indicators** related to :
 - The **vertical accuracy and precision** (correctness) of the altimetric measurements, i.e., indicators of the ability of the whole L1A-L3 system to “accurate” RWL measurements
 - The **temporal sampling** of the resulting L3 RWL time series, i.e., indicators of the ability of the whole L1A-L3 system to produce data for each satellite overflight over the river



3 Analysis of Case Study Output

In this section, we report on the outcomes of Validation exercise done at L3, but also for the outputs of each processing steps of the L3 processor: Step A: after water masking, Step B: after outliers rejection and Step C: after OPO selection.

3.1 Technical / Scientific Results

The objective of this Case Study is, *in fine*, to produce high quality L3 river water level data, starting from Sentinel-3A L1A and implementing processing configuration options that are optimised for the Inland Water conditions.

With regards to the objectives, Fig. 11 shows very satisfying L3 river water level time series resulting from the two configurations #1 and #2 with relatively low RMSE of 0.12 m and 0.13 m respectively. The error of the L3 SARM are about one order of magnitude smaller than those of L3 LRM data from Jason-2 (LRM) PISTACH project [RD-14] on the same place (year 2008, cf. Fig. 12) and subsequent study [RD-13].

Another interesting comparison can be done with results from the validation of CryoSat-2 ESA L2 SARM & SARINM data (Baseline B) [RD-15] that has been in the frame of the SHAPE Project (in order to demonstrate validation capability for geodesic orbit missions). In this study, L3 “pseudo time series” have been estimated exactly on the location of the Parintins gauging station used in this DeDop Case Study. The error values were as follows: For SAR mode: RMSE=1.04 m (0.91 ± 0.50 m), period 2010–2012 ; for SARINM RMSE=1.24 m (1.15 ± 0.46), period 2012–2015. Such different results for L3 derived from SARM acquisitions are surprising and need further investigation. In particular, ATK will update CryoSat-2 validation results over the Amazon thanks to the forthcoming release of the Baseline D data. However Baseline B results were also far better for other places along the Amazon river, e.g., SARM: 0.48 m (0.42 ± 0.23 m), SARINM: 0.86 m (0.77 ± 0.36 m).

Nonetheless, comparison to CryoSat-2 Baseline B results have to be interpreted with care since:

- RMSE encompasses for both Mean and STD of the measurement errors. For example, CryoSat-2 Baseline B data are degraded by high systematic bias errors but exhibits lesser errors in terms of STD alone, with values of ± 0.50 m for SARM and ± 0.46 m for SARINM.
- The amplitude of the variations of the Amazon river can vary by several metres from one year to another, challenging the ability to obtain comparable results for non-contemporary data.

The following sections dive into some more detailed analysis w.r.t. L1BS, L1B and L2 processing, focusing on cycle 29 during which some specific phenomena have been identified.

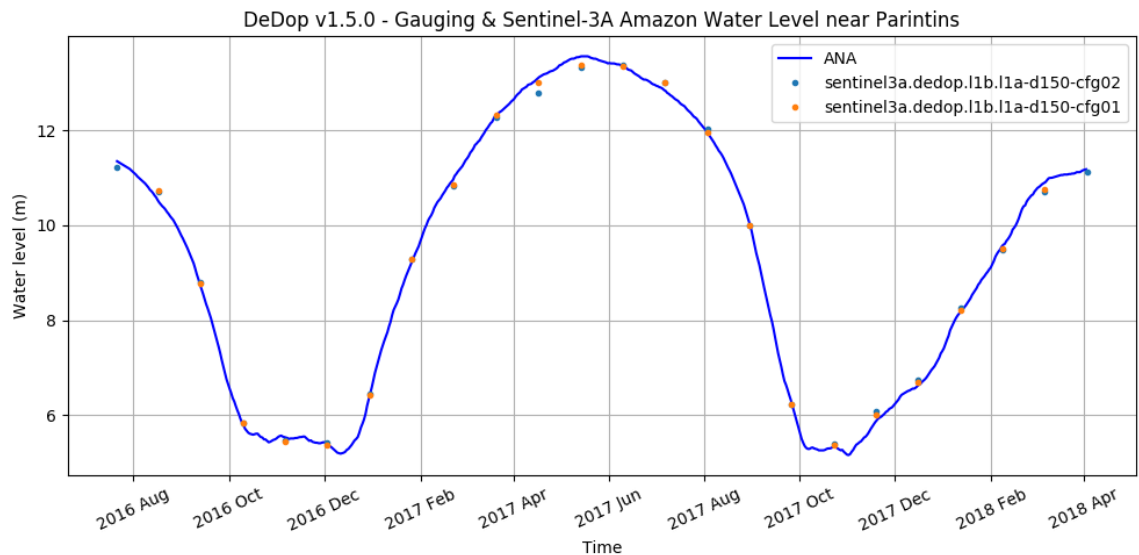


Figure 11. Sentinel-3A Amazon L3 River Water Level time series with gauging data.

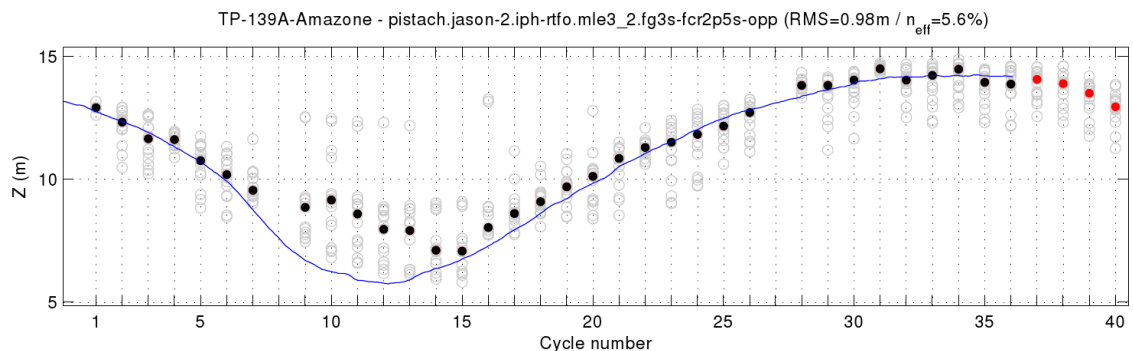


Figure 12. Jason-2 PISTACH/Ice3 time series close to Parintins town, track 139, year 2008
Extracted from [RD-14] document.

3.2 Impact of Different DeDop Processing Configurations

In this Case Study, and as discussed in section 3.3, there are no significant results between the tested configurations when analysed at L3 (cf. Table 3). However, there are important differences in the shape of the retrieved waveforms in the L1B and thus in the distribution of water level values derived from L2 retracking.

Fig. 13 provides the radargrams for cycle 29 for the two tested configurations #1 and #2 for which hyperbolic signature from side lobe echo lead Ice1g retracker to retrack shorter range values in configuration #1 while off-nadir and strong reflectors lead Ice1g retracker to retrack longer range values in configuration #2.

The impact of the DeDop configuration options is very important: randargram for configuration #1 exhibits lots of echoes before the leading edge of the waveforms:



these are signatures coming from strong reflectors caught by delay-Doppler side lobes. These effects disappear in the radargram for configuration #2 thanks to the Hamming windowing.

On the other hand, right over the Amazon river, around -2.6° latitude, we can see some off-nadir effect causing Ice1 to retrack longer range values. This effect is visible in both radargrams, but the impact is very different for the two configurations. Actually, the error (against gauging data) of the associated water levels derived from these Ice1 retracker are $RMSE\#1=5.10\text{ m}$ ($0.32\pm5.09\text{ m}$) and $RMSE\#2=3.63\text{ m}$ ($-1.76\pm3.18\text{ m}$), which are huge errors, they also include very different systematic bias and STD values. Configuration #1 has lower systematic bias due to the (insane!) compensation of both side lobe and off-nadir effects.

Analysis and validation results that have been done at intermediate processing stages in the L1A \rightarrow L1BS/L1B stack has showed some interesting facts and questioning:

- **Hamming windowing:** Despite being a very useful technique to clean up the SARM waveforms from side-lobe effects in case of specular surfaces, this windowing technique must be considered temporary while no other technique is able to **use Stack data as it is**, that is with no information loss. Actually, undesired effects such as those induced by delay-Doppler side-lobes are not noise at all: this is information we just cannot make benefit from for the time being.
- **Zero-padding:** During the development of this Case Study has been questioned the interest of **Zero Padding Factor > 1** (ZPF) when empirical retracker (like Ice1) are in use, as this is the case in here. This is because Zero-padding is aimed at refining waveforms sampling for physical models to better fit waveforms.

As a matter of facts, ALONG-TRACK S.A.S. has processed an alternate version of configuration #1 with $ZPF=2$. It turned out that this degraded Ice1 retracker outputs since this led to retrack an increased number of peaky echoes originating from side-lobes than with $ZPF=1$. However, this analysis might be valid only for this case study and its representativity is questionable. Finally, experience on sea ice surfaces revealed that $ZPF=2$ improved retracking results both empirical and physical retracker types [RD-16].

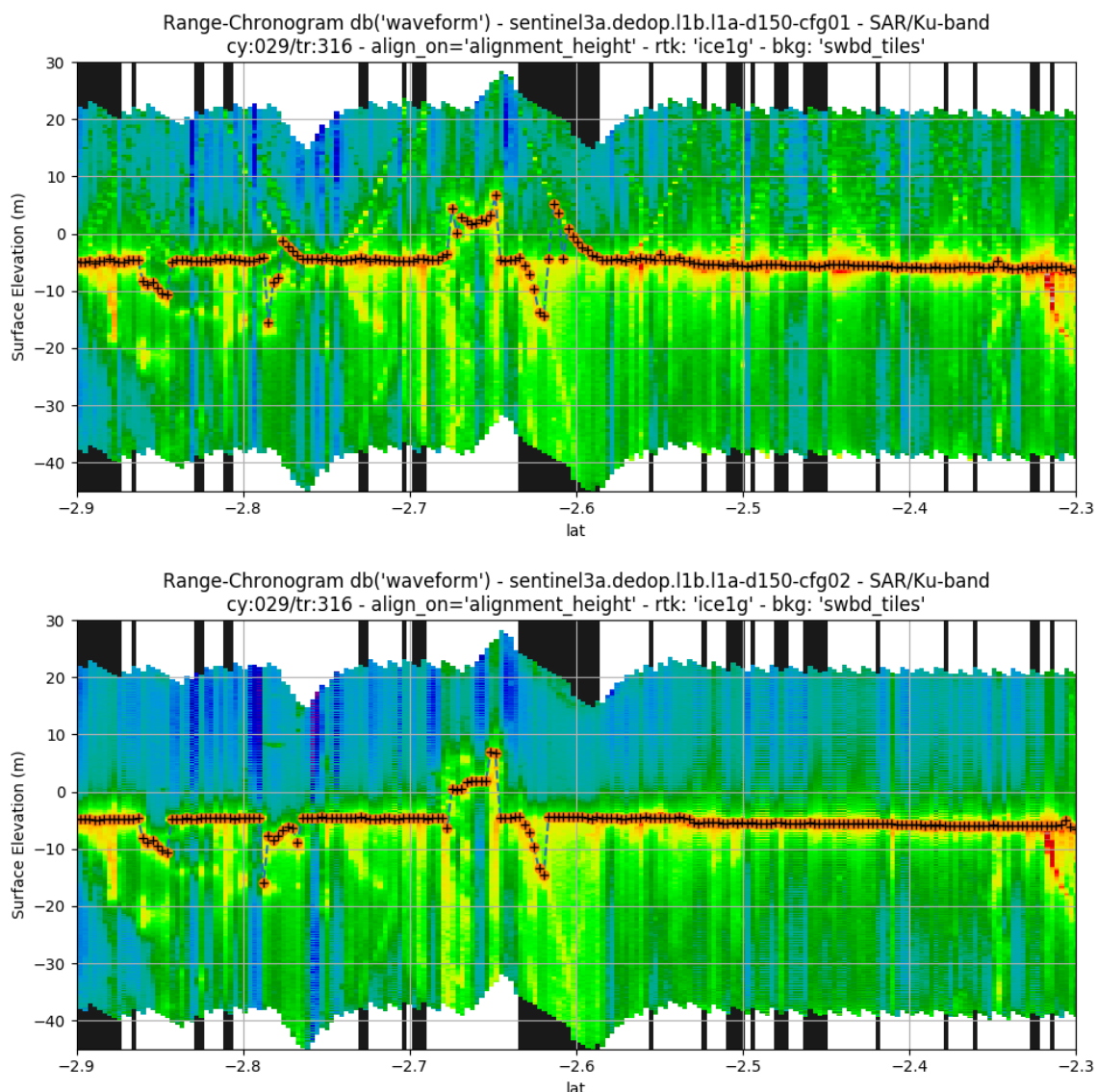


Figure 13. L1B/L2 Processors – Sentinel-3A L1B geophysical radargrams with Ice1 outputs (Top) Radargram for configuration #1 and (bottom) #configuration #2, cycle 29track 316. Both radargrams have Ice1g retracker outputs superimposed (black '+' in orange dots). Vertical black patches in the background mark altimetry records acquired into the SWBD water mask. Crossing over the Amazon river the corresponds to the large black patch @-2.6° latitude.

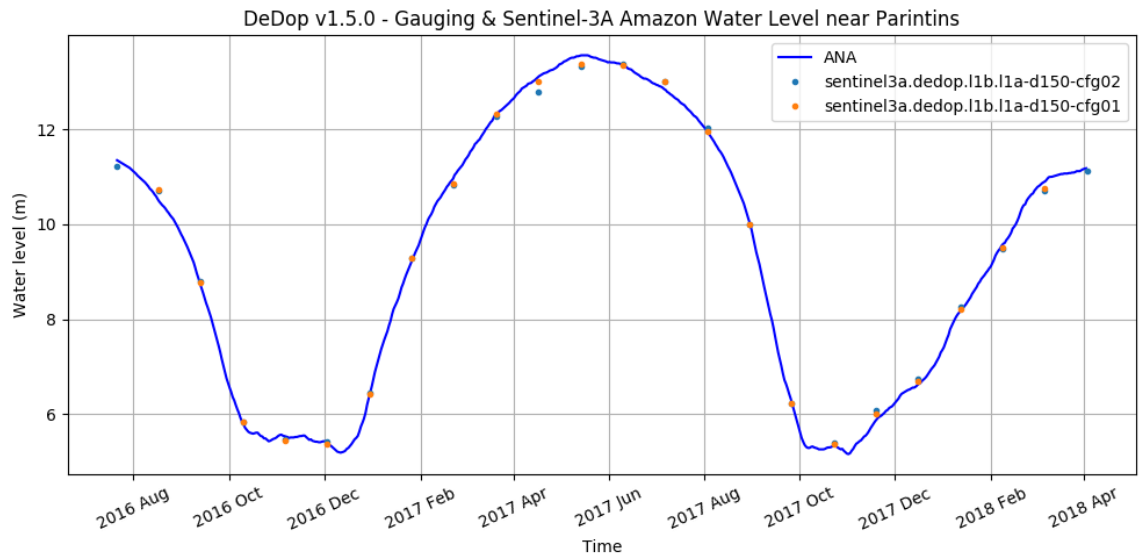
3.3 Product Validation Report

3.3.1 L3 Validation Results

The Validation exercise has been applied on time series of river water levels, that are provided by the L3 Processor. Fig. 14 (top) illustrates the water level time series of the Amazon river at Parintins and Fig. 14 (bottom) provide time series of the



measurement errors. The results are very encouraging with relatively low RMSE of 0.12 m and 0.13 m for the two configurations, respectively #1 and #2.



Sentinel-3A Amazon L3 River Water Level time series with gauging data. (replication of Fig. 11 for convenient visualisation together with error time series below).

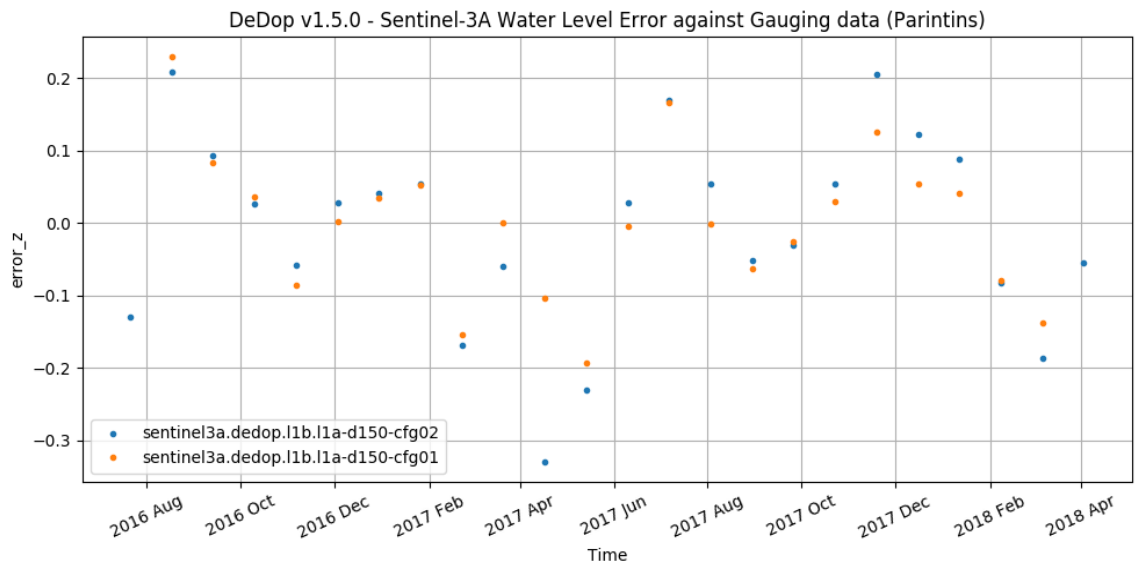


Figure 14. Sentinel-3A Amazon Error time series of L3 Water Level (Orange) Error for configuration #1 – (Blue) Error for configuration #2.

Table 3 summarises all validation results for the various processing steps that occur within the L3 Processor, as illustrated in Fig. 10.



Table 3. Validation results for the L3 River Water Level time series.
Detailed results for all steps of the L3 Processor, including: (A) L2 in water mask, (B) Outlier rejection and (C) final L3 for the two configurations #1 and #2.

L3 Processing Step	DDP Config	Nb meas.	Mean±STD (m)	RMSE (m)	Sampling Loss Rate (%)
Step A. L2 – All records in Water Mask	#1	422	- 0.14±3.34	3.34	<i>N.A. (SLR defined for L3 data only)</i>
	#2	422	- 0.61±2.60	2.66	
Step B. L2 – After outliers rejection filter	#1	380	0.11±1.91	1.92	
	#2	377	- 0.07±0.40	0.41	
Step C. L3 – Final: After OPO routine (median meas.)	#1	24	0.01±0.12	0.12	0%
	#2	24	- 0.01±0.13	0.13	0%

3.3.2 Discussion on the L3 validation results

L3 Validation results, for the two DeDop configurations, are very close to each other, differing by one centimetre only: RMSE#1 is 0.12 m (0.01±0.12 m) while RMSE#2 is 0.13 m (- 0.01±0.13 m). Such a small difference is usually considered meaningless over Inland Water (LRM context) for which usual error values range from few centimetres (rare cases) to tens of centimetres (most of the cases) or even meters in worse cases [RD-6].

It is worth noting that both configurations exhibit no data loss with null values for the Sampling Loss Rate (SLR) indicator, indicating that data from all cycles have been processed successfully. Such results are excellent but normal since Jason-2 and ENVISAT satellites for which SLR values were very small (about 5 % at maximum) and null otherwise.

Considering the important differences between configuration #1 and #2 found in both L1B (radargrams) and L2 (retracked ranged) outputs and the very high quality results for the two configurations of the L3 outputs, further analysis from within the L3 Processor were required. They are reported in Table 3 and graphically represented in Fig. 15. The validation routines have been run for all of the measurements outputted after each of A, B and C steps of the L3 Processor. The conclusions are very clear: the L3 Processor is able to produce very high quality data, starting from L2 data of different quality. This is for this crossing over the Amazon and shall be demonstrated for others as well in SARM.

We can conclude that the amplitude of the measurement errors at L2 has a limited impact on the L3 Processor's outputs. However, this is true for this specific crossing over the Amazon river but might degrade for other locations or other rivers due to greater contamination at L1BS, L1B and thus at L2.

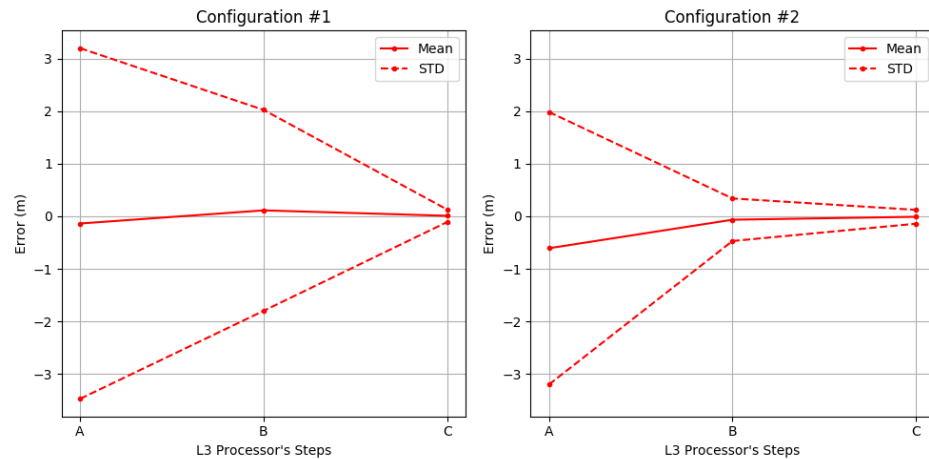


Figure 15. L3 Processor – Error evolution through the processing steps A, B and C
Step A: after water masking, Step B: after outliers rejection and Step C: after OPO selection =
Final L3 data. Please refer to Table 3 to read numerical values.

As a general picture, experience from ATK is that the L3 Processor performs well whenever input L2 data do not contain extremely erroneous water level outsiders and when the L2 data from within the water mask (prior Step A) have reasonable dispersion, typically lesser than the amplitude of the hydrological signal itself.

3.4 DeDop Processor and Tool Performance

This sections provides discussion on the following topics:

- Section 3.4.1 DeDop Processor
- Section 3.4.2 DeDop Core Performance
- Section 3.4.3 Technical Recommendations
- Section 3.4.4 ATK's contribution to DeDop source code: `ecef2lla()` function
- Section 3.4.5 ATK's add-on to DeDop Core: `dedop_run_scheduler`

3.4.1 DeDop Processor

Part of the recommendations suggested by ATK at proposal time was to produce a tool that can be used in some automated manner, with a special focus on these two points:

1. Be able to **run DeDop from the shell command line**: this is actually perfectly embodied by the DeDop Core tool and fully exploited by the job scheduler developed by ATK.
2. Be able to **interface DeDop routines into in-house programs**: this is perfectly satisfied by the choice of extremely versatile and science-friendly Python programming language.



In this study, ATK only made use of the DeDop Core tool.

3.4.2 DeDop Core Performance

Details on DeDop Core performances are provided as part of section 2.4.2.2.

3.4.3 Technical Recommendations

ATK technical recommendations for the future of DeDop tools are as follows:

1. **L1A Geo-selection:** Since Sentinel-3 L1A product files are pole-to-pole, it would be very useful to be able to reduce the list of L1A data records to be processed to those included into a geographical bounding box.
2. **Parallelised processing:** Make DeDop able to natively process L1A files in parallel. However since this is solved by [dedop_run_scheduler](#) open source tool from ATK, this item is of lesser priority.
3. **L2 components:**
 - **Retracker:** Integration of a retracker to DeDop, e.g., starting with Ice1 would be a fair choice. ATK is considering the possibility to contribute with its in-house implementation of the Ice1 retracker.
 - **L2 Corrections:** Integration of basic atmospheric and geophysical corrections such as: iono, wet/dry tropo and barometric corrections, pole & surface tides, etc.

3.4.4 ATK's contribution to DeDop source code: ecef2lla() function

During the development of this Case Study, [ecef2lla\(\)](#) routine was not converging for some product files, making DeDop to enter infinite loops and never stop. In response to this issue, ATK has been able to track down the problem through the source code and has proposed an alternate implementation to the [ecef2lla\(\)](#) routine. The routine submitted by ATK has been integrated and is now part of the official DeDop codebase.

3.4.5 ATK's add-on to DeDop Core: dedop_run_scheduler

For the needs of this Case Study, ATK had to run DeDop Core numerous times. However, by 2016-2018, initial runs based on CryoSat-2 L1A data took about 16 hours each on ATK processing facility (Intel Core i7 CPU with 8 logical cores, 16GB ram, SSD drive).

In order to reduce the strong overhead impacted by long computational time, ATK has developed a job scheduler able to run DeDop Core instances on several logical cores in parallel. The computational speed up resulting from this tool is equal to the number of logical cores that the users can allocate to DeDop Core instances.



This scheduler, [dedop_run_scheduler](#), is an open source bash shell script. It has been made available on GitHub.com⁴ on March 12th 2018. It can be used on operating systems able to run both the bash shell and the DeDop Core (e.g., Linux and MAC OSX among others). It should also run well on Windows 10 machines equipped for example with the Linux User Space, developed in a joint effort by the Ubuntu project and Microsoft⁵.

4 Conclusions / Recommendations

In this section, we report on Case Study conclusion and recommendations.

4.1 Conclusions

For this Case Study over Inland Water, the DeDop Core v1.5.0 open source software has been implemented successfully, in order to produce L1B (and L1BS data products unused in this study) starting from Sentinel-3A L1A product files obtained from the Copernicus/SciHub web portal.

The high flexibility and configurability of the DeDop Core tool allowed to fine tune various aspects of the delay-Doppler processing for the specific needs and challenging case of inland water surfaces. The DeDop Core tool has been run for two different configurations: **#1** meant to be a “basic SARM processing” and **#2** which is optimized for Inland Water.

The chosen study area is at the crossing of Sentinel-3A track 316 and the Amazon river (downstream section), close to Parintins town from which in situ gauging data are available⁶.

In order to make DeDop even more productive, ALONG-TRACK S.A.S. has contributed a free and open source tool, named [dedop_run_scheduler](#), that allows to run DeDop Core in parallel jobs on multi-core machines (i.e., one input L1A file processed per CPU core). Computational time are then be considerably reduced.

ALONG-TRACK S.A.S. has contributed a small but important patch to DeDop source code in order to solve and close **Issue #31** on the GitHub issue tracker (alternate implementation of the `ecf211a()` function).

On top of DeDop Core, ALONG-TRACK S.A.S. has set up a full L2 → L3 processing stack in order to produce water level time series derived from altimetry and to validate them:

1. **Add-on L2 Processor:** Empirical retracker (“Ice1g”, fast and custom ALONG-TRACK’s implementation of Ice1), corrections & geoid model,

⁴ Script is available from GitHub.com: https://github.com/nbercher-atk/dedop_run_scheduler.

⁵ Cf. <https://docs.microsoft.com/en-us/windows/wsl/about> and <https://blog.ubuntu.com/2016/03/30/ubuntu-on-windows-the-ubuntu-userspace-for-windows-developers>.

⁶ Sentinel-3A cycles 5 – 36 have been processed, however due to lack of gauging data, only cycles 5 – 29 have been validated.



2. **Add-on L3 Processor (Alti-Hydro tools):** read & geo-select L2 data within water mask, outlier measurements rejection, production of final L3 water level time series,
3. **Add-on Validation tools:** L3 data quality quantification against collocated & codated in situ gauging data.

Analysis and validation results that have been done at intermediate processing stages in the L1A → L3 processing stack. This has raised some interesting comments and questioning about, e.g., the relevance of Hamming windowing, and Zero Padding in conjunction with empirical retrackers.

Despite no significant quality of the validated products can be observed at L3 for this specific crossing over of Amazon river, it is clear, and as expected, that the ability to customise the delay-Doppler processing of L1BS and/or L1B SARM is very beneficial for the case of Inland Water.

The overall quality of the L3 products generated and validated in the frame of this Case Study can be considered very good in comparison to the performances of previous missions [RD-6]:

- **Basic Configuration #1:** **RMSE#1 = 0.12 m (0.01±0.12 m)**
- **Inland Water configuration #2:** **RMSE#2 = 0.13 m (- 0.01±0.13 m)**

4.2 Recommendations

The most important recommendation from ALONG-TRACK S.A.S. is not technical, but rather managerial. It is about maintaining a perennial development leadership on the DeDop source code after the end of the ACA-DDP project.

Actually, DeDop as an open source project has very limited audience due to its very specific application domain, if compared to well known open source projects. As such, **it is important to realise that the DeDop code base will soon be in a fragile situation if no specific actions are taken to ensure proper maintenance and continuation right after the end of the ACA-DDP project.** This recommendation is of major importance to start set up with no delay a group of developers, maintainers & leader(s) that would:

- Drive the vision for the future of DeDop
- Maintain the various DeDop tools
- Merge patches provided by users community
- Continue to improve the tool
- Communicate via ESA (and other agencies) about DeDop
- Keep training the young (and old!) generations of potential users

Other recommendations from ALONG-TRACK S.A.S. are:

- Organise trainings on the various DeDop tools, e.g., during events like ESA LPS, OSTST, Coastalt workshops, 30YRA, etc.
- Make DeDop able to run files in parallel.
- Continue the good work!



5 Acronyms and Definitions

The content of these subsections were kindly made available by the SHAPE project⁷ team.

5.1 Acronyms

AD	Applicable Documents	GDR, [I-,S-]	Geophysical Data Record, [Interim-, Scientific-]
AGC	Automatic Gain Control	GFZ	Deutsche GeoForschungsZentrum (German Research Centre for Geosciences)
AH	Alti-Hydro	GOCE	Gravity field and steady-state Ocean Circulation Explorer
AHP	Alti-Hydro Product(s)	GPOD	Grid Processing on Demand
ANA	Agência Nacional de Águas (National Water Agency, Brazil)	GPP	Ground Processing Processor
AoA	Angle of arrival	GPS	Global Positioning System
API	Application Programming Interface	GRACE	Gravity Recovery And Climate Experiment
ATK	ALONG-TRACK S.A.S.	GRGS	Groupe de Recherche de Géodésie Spatiale (Space Geodesy Research Group)
AVISO	Archivage, Validation et Interprétation des données des Satellites Océanographiques	IE	Individual Echoes
CoG	Centre of Gravity	IPF	Integrated Processing Facility
CPP	CryoSat-2 Processing Prototype (CNES)	ISD	isardSAT
CryoSat-2	Altimetry satellite for the measurement of the polar ice caps and the ice thickness	IRF	Impulse Response Function
CRUCIAL	CRYosat-2 sUccess over Inland wAtter and Land	Jason-1	Altimetry satellite, T/P follow-on
DDM	Delay-Doppler Map	Jason-2	Altimetry satellite, also known as the « Ocean Surface Topography Mission » (OSTM), Jason-1 follow-on
DDP	Delay-Doppler Processor	Jason-3	Altimetry satellite, Jason-2 follow-on
DEM	Digital Elevation Model	Jason-CS	Jason Continuity of Service
DGC	Doppler Ground Cell	KML	Keyhole Markup Language
DTC	Dry Tropospheric Correction	KO	Kick Off
DTU	Danmarks Tekniske Universitet (Technical University of Denmark)	L1A	Level-1A
EGM	Earth Gravitational Model	L1B	Level-1B
ENVISAT	ENVironment SATellite	L1BS	Level-1B-S (aka, Stack data)
EO	Earth Observation	L2	Level-2
ESA	European Space Agency	L3	Level-3
FBR	Full Bit Rate	L4	Level-4
FR	Final Review (meeting)	LEGOS	(french acr.) Laboratoire d'Études en Géophysique et
FR	Final Report (document)		
FTP	File Transfer Protocol		

⁷ <https://projects.along-track.com/shape/>



	Océanographie Spatiale (Laboratory for Studies in Geophysics and Spatial Oceanography)	SCOOP	for Ocean Research & Exploitation
LOTUS	Preparing Land and Ocean Take Up from Sentinel-3	SEOM	SAR Altimetry Coastal & Open Ocean Performance
LPS	Living Planet Symposium	SHAPE	Scientific Exploitation of Operational Missions
LRM	Low Resolution Mode		Sentinel-3 Hydrologic Altimetry PrototypE
LSE	Least Square Estimator	SME	Small and Medium-sized Enterprise
LWL	Lake Water Level		Statement Of Work
LWS	Low Water Stage	SOW	Sentinel-3 Surface Topography Mission System Performance Simulator
MTR	Mid Term Review	SPS	
MSS	Mean Sea Surface		
MWR	Microwave Radiometer		
netCDF	Network Common Data Form	SRAL	SAR Radar Altimeter
NOAA	National Oceanic and Atmospheric Administration	Stack	Matrix of stacked Doppler beams
OCOg	Offset Centre of Gravity	STD	Standard Deviation
OPO	One per Overflight	STM	Sentinel-3 Surface Topography Mission
OSTM	Ocean Surface Topography Mission (also known as Jason-2), is also the name of the satellites series T/P, Jason-1, Jason-2 and Jason-3	SWBD	SRTM Water Body Data
		TAI	Temps Atomique International (International Atomic Time)
PRF	Pulse Repetition Frequency	TBC	To Be Confirmed
PTR	Point Target Response	TBD	To Be Done
RD	Reference Document	TN	Technical Note
RDSAR	Reduced SAR (also known as Pseudo-LRM)	T/P	Topex/Poseidon (altimetry satellite)
		URL	Uniform Resource Locator
RIP	Range Integrated Power (of the MLD) sometimes referred as Angular Power Response (APR)	USO	Ultra Stable Oscillator
		UTC	Coordinated Universal Time
RMS	Root Mean Square	UWM	Updated Water Mask
ROI	(geographical) Region(s) Of Interest	VS	Virtual Station(s)
		VH	Vertical-Horizontal polarisation
RWD	River Water Discharge	VV	Vertical-Vertical polarisation
RWL	River Water Level	WBS	Work Breakdown Structure
SAMOSa	SAR Altimetry MOde Studies and Applications	WFR	Water Fraction Ratio
		WM	Water Mask
SARAL	In Indian "simple", in english "SATellite for ARgos and AltiKa.	WP	Work Package(s)
		w.r.t.	with respect to
SARIN	SAR Interferometric (CryoSat- 2/SIRAL mode)	WTC	Wet Tropospheric Correction
		XML	eXtensible Markup Language
SAR	Synthetic Aperture Radar	ZP	Zero Padding
SARvatore	SAR Versatile Altimetric Toolkit	ZPF	Zero Padding Factor



5.2 Definitions

5.2.1 In Altimetry

Level-0 (L0) : Raw Data.

Level-1A (L1A) : Unpacked L0 complex echoes that have been sorted and calibrated. Geo-location information is also included. Product relevant to SAR processing specialists allowing fundamental studies on SAR processing such as Doppler beam formation and for calibration studies using ground-based Transponders.

Level-1B-S (L1B-S) : Geo-located, calibrated azimuth formed complex (I and Q) echoes related to a given location on the ground, after slant range correction. No averaging of individual waveforms (i.e. multi-looking/stacking) is applied. Relevant ancillary data (e.g. beam angles, calibration information, statistical description of the multi-looked data etc.) is included. Product relevant to geophysical retrieval algorithm developers (over ocean, land and ice surfaces), surface characterisations studies (e.g. impact of sea state bias, wave directional effects etc.) and Quality Control systems.

Level-1B (L1B) : Geo-located, calibrated, azimuth formed, slant range corrected and averaged together (i.e. multi-looked/stacked) power echoes associated with a fixed point on the ground-track. This product is relevant to geophysical retrieval algorithm developers and Quality Control systems.

Repeat Period : The time elapsed between two revisits of a satellite on the same ground track location. The repeat period is noted T_{sat} .

5.2.2 In Alti-Hydrology

Alti-Hydrology refers to the radar altimetry techniques dedicated to the production, verification and validation of high quality level water products (so called Alti-Hydro Time Series). River discharge may be later derived from the water level time series.

Alti-Hydro Time Series are time series of water level (of river or lake) or river discharge constructed from Radar Altimetry measurements which are collected at a Virtual Station.

Alti-Hydro Products are one or more Alti-Hydro Time Series.

Effective Sampling Period, noted T_{eff} , is the mean temporal period of an Alti-Hydro Time Series. It is greater (degraded cases) or equal (nominal case) to T_{sat}/N_{sat} , i.e., the satellite orbit repeat period (T_{sat}) divided by the number of tracks (N) crossing the water body (N is 1 or 2 for rivers and $N \geq 1$ for lakes).

Geodetic Orbit, in the context of Alti-Hydrology, means an orbit whose repeat period is much higher than the period of a Repeat Orbit, and which does not permit to correctly sample, at least, the annual variations of surface water level (typically $T_{sat} > 365/4$ days).



High Water Stage, for a discrete time series, is defined as the set of water level measurements included in the temporal interval that embraces the 1/3 of the highest values of the in situ measurements of the whole time series. High Water Stage defines time intervals based on the repartition of measurements population and is not to be confused with the top 1/3 of the water level amplitude.

Low Water Stage, for a discrete time series, is defined as the set of water level measurements included in the temporal interval that embraces the 1/3 of the lowest values of the in situ measurements of the whole time series. Low Water Stage defines time intervals based on the repartition of measurements population and is not to be confused with the bottom 1/3 of the water level amplitude.

Migration of Altimetry Measurements is a methodology used to migrate altimetry measurements of water level along the river path (or over a lake surface), from the **geodetic** spatio-temporal sampling pattern of a geodetic altimetry mission (such as CryoSat-2) to the one of a shorter repeat period (such as Sentinel-3). The results are called Pseudo Time Series.

The methodology is also used to migrate altimetry measurements of water level along the river path to locations corresponding to in situ stations or hydrological model sub-basin outlets, for the purpose of validation and assimilation, respectively.

Pseudo Time Series are emulated water level time series constructed from Spatio-Temporal Series in order to be able to mimic the traditional repeat track techniques usually implemented, at Virtual Stations or on lake surfaces, on classic water level time series (i.e., from orbit of repeat period $\ll 365$ days). Pseudo Time Series are built using measurements migration techniques.

Quality of Water Level and discharge Products:

- For **Water Level Products**: is the association of measurements **Correctness** along with the **Sampling Loss Rate** to give an image of the overall ability of the Altimetry System to produce water level values.
- For **Discharge Products**: is defined by the measurement correctness estimated by statistical indicators such as root-mean-square error, Nash-Sutcliffe model efficiency coefficient, Kling-Gupta efficiency, and more qualitative indicators based on water balance realism (Bodyko framework), as well as delay propagation error.

Repeat Orbit, in the context of Hydrology from Space, means an orbit whose repeat period is much lower than one year (thus $T_{sat} \ll 365$ days).

Sampling Loss Rate, or SLR (noted η_{eff}) is, for Alti-Hydro time series, the ratio of the number of measurements lost by the Altimetry System on the nominal number of measurements. It is linked to the **Effective Sampling Period** T_{eff} by the following relation:

$$\eta_{eff} = 1 - \frac{N_{eff}}{N_{sat}} = 1 - \frac{T_{sat}}{T_{eff}}$$



with N_{sat} and N_{eff} being, respectively, the number of nominal measurements and the number of acquired measurements; T_{sat} and T_{eff} being, respectively, the number of nominal sampling period and **Effective Sampling Period**.

For instance, Sentinel-3 products should be characterised by $T_{sat}=27$ days (13.5 measurement per year) at a single-track Virtual Station. If it is to provide only 6.75 measurements per year (that is $T_{sat}=54$ days), then its sampling loss rate would be 50%.

Spatio-Temporal Series or space-time series are series of water level measurements collected along a river path (space x) at various instants (time t), typically, but not only, from a satellite flying on a geodetic orbit (of long repeat period). Spatio-Temporal Series are bi-dimensional data by nature, noted $Z(x,t)$.

Validation is the process of **quantifying measurements error** and **deriving measurements error statistical indicators**. That is, a **trusted reference** of the measured variable must be available (i.e., adequately collocated) to compute the **measurement error** (water level or discharge). Validation can be achieved on river and lake water level as well as river discharge against in situ data (the reference), altogether collocated in space **and** time.

- In case of water level time series, together with measurement error statistical indicators, the **sampling loss rate** (defined later in this section) constitute the ensemble of **Quality Indicators**.
- In the case of river discharge, we propose to compute **measurement error statistical indicators** such as root-mean-square-error, relative volume error, mean and standard deviation error, and correlation; summarizing statistical indicators such as the Kling-Gupta efficiency; as well as **propagation delay error**.

Verification is the process of giving **qualitative indicators about the measurements quality** without collocated (in space, time, nor both) reference data. This can be done by comparing **seasonal trends** of the measured variable to the seasonal trends of **past and present reference archives**. The reference datasets can be in situ or altimetry-derived data (for water levels) and in situ river discharge. But expertise must ensure that the depicted trends are adequate enough in respect to the observed water body, its morphology and hydraulic dynamics, versus reference data location and acquisition dates. Generally speaking, **Validation is preferred against Verification** whenever collocated in situ data are available.

Virtual Station is a location, along a river path, where one or two satellite tracks cross the river.

Water mask : Thematic map layer of boolean values indicating the presence, or not, of water. Water masks are usually derived from satellite imagery and can be divided in two families : (1) “gridded masks” : grids of individual pixel values (usually released as raster GIS formats) or (2) “object masks” : grouped pixels derived from object-oriented segmentation and classification techniques from which polygons may be derived (usually released as raster images or vectorized formats, e.g., ShapeFiles).



5.2.3 In Hydrology

Lake Level (m) is the Water Level in a lake relative to a specified datum. This variable is one of the Terrestrial Essential Climate Variables (T04) defined by GCOS.

Reach (river), or section : sub section along a river defined by an inlet section and an outlet section.

River Discharge (m^3/s) is the volume rate of water flow (including any suspended solids, dissolved chemicals, and/or biologic material, etc.) which is transported through a given cross-sectional of a river. This variable is one of the Terrestrial Essential Climate Variables (T01) defined by GCOS.

River Profile (m) is the longitudinal height of the water line, at given time or related to any other concept (e.g., high water stages). This is a driving parameter to the estimation of river discharge (slope) and altimetry data migration along the river path. The river profile is also the integral of the river longitudinal slope (river slope).

River Slope (m/km) is the slope of the water line of a river, along its longitudinal direction. The river slope is also the first order derivative river profile.

Semi-distributed model: In a semi-model distributed model, some processes are modelled by dividing a watershed into several sub parts. This space subdivision can be driven by various hydrological (e.g., sub watersheds) or topological constraints (e.g., height intervals). Such models help to take in account for the spatial variability of the processes to be modelled.

Water level (m), also known as **Water stage** or **Gauge Height**, is the altitude of the free surface of a stream (river), lake or reservoir relative to a specified datum⁸.

Watershed, catchment or drainage basin is an extent or an area of land where surface water from rain, melting snow, or ice converges to a single point at a lower elevation. In other words, this single point suffices to define the watershed extent.

5.2.4 In Experimental Science

Resolution : the smallest variation of the physical parameter to be measured that induces a change of value at the instrument : it results from the combination of the instrument sensitivity and the number of bits of the quantizer (sample size).

Accuracy (or systematic bias) is the distance between the average of the measurements and the true value, it gives an information on the degree of closeness of measurements of a quantity to that quantity's actual (true) value.

Precision : the mean distance between the measurements themselves and their mean value (i.e., the standard deviation of the random variable that models the measurement experiment). It is related to reproducibility and repeatability, is the degree to which repeated measurements under unchanged conditions show the same results.

8 Please note that we are generally talking of water level as height (i.e., above the geoid) instead of as elevation (i.e., above the ellipsoid). Users and Readers should therefore keep in mind that they have to check that the same geoid model and version have been used when comparing / merging various water level products.



ALONG-TRACK
.com

Project ref.: DeDop_ESA_TN_023

Issue: 0.5

Date: 2019-05-15

Page: 41 of 49

Correctness is the junction of both accuracy and precision. A measurement system can be accurate but not precise, precise but not accurate, neither, or both. For example, if an experiment contains a systematic error, then increasing the sample size generally increases precision but does not improve accuracy. The result would be a consistent yet inaccurate string of results from the flawed experiment. Eliminating the systematic error improves accuracy but does not change precision. A measurement system is considered valid or correct if it is **both accurate and precise**.



ALONG-TRACK
.com

Project ref.: DeDop_ESA_TN_023

Issue: 0.5

Date: 2019-05-15

Page: 42 of 49

6 Annex A. Presentation of Case Study: “Inland Water Processing of Sentinel-3 L1A SARM data with DeDop Core”

Annex A is delivered with the present report in the form of presentation slides:

ATK document ref: **ATK_ESA_ACADDP_SLIDES_2019_008**

Issue: **1.0**

File: ATK_ESA_ACADDP_SLIDES_2019_008_WP6400_Inland_water_case_study.pdf



7 Annex B. DeDop configuration files

This section provides complete content of the DeDop configuration files (excluding characterisation & constant files).

7.1 Configuration file #1: Basic SARM

Content of file **CNF.json**:

```
{
  "__metainf__": {
    "description": "DeDop Configuration File",
    "version": 3,
    "changelog": [
      {
        "version": 0,
        "parameters": [],
        "comment": "initial version"
      },
      {
        "version": 1,
        "parameters": [
          ["flag_azimuth_processing_method_cnf", "*", "integer codes changed to text enum"]
        ],
        "comment": "Update to azimuth processing method flag"
      },
      {
        "version": 2,
        "parameters": [
          ["flag_cal2_table_index_cnf", "+", "added CAL2 table index"]
        ]
      },
      {
        "version": 3,
        "parameters": [
          ["output_format_flag_cnf", "+", "new optional parameter"],
          ["flag_remove_doppler_ambiguities_cnf", "-", "removed unused parameter"],
          ["ambiguity_mask_margin_cnf", "-", "removed unused parameter"],
          ["elevation_reference_value_cnf", "-", "removed unused parameter"]
        ],
        "comment": "added option for selecting output format"
      }
    ]
  },
  "flag_cal2_correction_cnf": {
    "value": true,
    "units": "flag",
    "description": "Flag that activates the CAL2 corrections: Deactivated (false); Activated (true)"
  },
  "flag_uso_correction_cnf": {
    "value": true,
    "units": "flag",
    "description": "Flag that activates the USO correction: Deactivated (false); Activated (true)"
  },
  "flag_cal2_table_index_cnf": {
    "value": 2,
    "units": null,
    "description": "CAL2 table index, one of [0, 1, 2] (default: 2)"
  }
}
```



```
,
"flag_call_corrections_cnf": {
  "value": true,
  "units": "flag",
  "description": "Flag that activates the CAL1 corrections: Deactivated (false);
Activated (true)"
},
"flag_call_intraburst_corrections_cnf": {
  "value": true,
  "units": "flag",
  "description": "Flag that activates the CAL1 intraburst corrections: Deactivated
(false); Activated (true)"
},
"flag_surface_focusing_cnf": {
  "value": false,
  "units": "flag",
  "description": "Flag that activates the surface focussing: Deactivated (false);
Activated (true)"
},
"surface_focusing_lat_cnf": {
  "value": 0.0,
  "units": "Degrees North",
  "description": "Location of the surface focusing target (latitude) (ignored unless
flag_surface_focusing_cnf is 'true')"
},
"surface_focusing_lon_cnf": {
  "value": 0.0,
  "units": "Degrees East",
  "description": "Location of the surface focusing target (longitude) (ignored unless
flag_surface_focusing_cnf is 'true')"
},
"surface_focusing_alt_cnf": {
  "value": 0.0,
  "units": "m",
  "description": "Location of the surface focusing target (altitude) (ignored unless
flag_surface_focusing_cnf is 'true')"
},
"flag_azimuth_processing_method_cnf": {
  "value": "approx",
  "units": "flag",
  "description": "Flag that indicates the azimuth processing method: Approximate
('approx'); Exact ('exact')"
},
"flag_postphase_azimuth_processing_cnf": {
  "value": false,
  "units": "flag",
  "description": "Flag that enables the post-phase azimuth processing: Deactivated
(false); Activated (true)"
},
"flag_azimuth_windowing_method_cnf": {
  "value": "none",
  "units": "flag",
  "description": "Flag the sets the azimuth windowing method: Disabled ('none');
Boxcar ('boxcar'); Hamming ('hamming'); Hanning ('hanning')"
},
"azimuth_window_width_cnf": {
  "value": 64,
  "units": "count",
  "description": "Width of Azimuth window (minimum value: 32, maximum value: 64)"
},
"flag_doppler_range_correction_cnf": {
  "value": true,
  "units": "flag",
  "description": "Flag that activates the Doppler range correction in the geometry
corrections: Deactivated (false); Activated (true)"
},
"flag_slant_range_correction_cnf": {
```



```
"value": true,
"units": "flag",
  "description": "Flag that activates the slant range correction in the geometry
corrections: Deactivated (false); Activated (true)"
},
"flag_window_delay_alignment_method_cnf": {
  "value": 0,
  "units": "flag",
  "description": "Flag to indicate the window delay alignment method: Surface dependent
(0); Beam max integrated power (1); Satellite position above surface (2); Look angle 0
(3); Doppler angle 0 (4)"
},
"flag_stack_masking_cnf": {
  "value": true,
  "units": "flag",
  "description": "Flag that activates the Stack Masking algorithm: Activated (true);
Deactivated (false)"
},
"flag_avoid_zeros_in_multilooking_cnf": {
  "value": true,
  "units": "flag",
  "description": "Flag that indicates if the samples set to zero in the beams will be
avoided when averaging in multi-looking: No (false); Yes (true)"
},
"flag_surface_weighting_cnf": {
  "value": true,
  "units": "flag",
  "description": "Flag that activates the surface weighting: Deactivated (false);
Activated (true)"
},
"flag_antenna_weighting_cnf": {
  "value": false,
  "units": "flag",
  "description": "Flag that activates the antenna weighting: Deactivated (false);
Activated (true)"
},
"zp_fact_range_cnf": {
  "value": 1,
  "units": null,
  "description": "Zero padding factor used during range compression"
},
"N_looks_stack_cnf": {
  "value": 240,
  "units": null,
  "description": "Number of looks in 1 stack"
},
"output_format_flag_cnf": {
  "value": "extended",
  "units": "flag",
  "description": "Flag that specifies output format: the DeDop extended format
('extended') or default Sentinel-3 format ('sentinel-3')"
}
}
```



7.2 Configuration file #2: SARM for Inland Water

Content of file **CNF.json**:

```
{
  "__metainf__": {
    "description": "DeDop Configuration File",
    "version": 3,
    "changelog": [
      {
        "version": 0,
        "parameters": [],
        "comment": "initial version"
      },
      {
        "version": 1,
        "parameters": [
          ["flag_azimuth_processing_method_cnf", "*", "integer codes changed to text enum"]
        ],
        "comment": "Update to azimuth processing method flag"
      },
      {
        "version": 2,
        "parameters": [
          ["flag_cal2_table_index_cnf", "+", "added CAL2 table index"]
        ],
      },
      {
        "version": 3,
        "parameters": [
          ["output_format_flag_cnf", "+", "new optional parameter"],
          ["flag_remove_doppler_ambiguities_cnf", "-", "removed unused parameter"],
          ["ambiguity_mask_margin_cnf", "-", "removed unused parameter"],
          ["elevation_reference_value_cnf", "-", "removed unused parameter"]
        ],
        "comment": "added option for selecting output format"
      }
    ]
  },
  "flag_cal2_correction_cnf": {
    "value": true,
    "units": "flag",
    "description": "Flag that activates the CAL2 corrections: Deactivated (false); Activated (true)"
  },
  "flag_uso_correction_cnf": {
    "value": true,
    "units": "flag",
    "description": "Flag that activates the USO correction: Deactivated (false); Activated (true)"
  },
  "flag_cal2_table_index_cnf": {
    "value": 2,
    "units": null,
    "description": "CAL2 table index, one of [0, 1, 2] (default: 2)"
  },
  "flag_cal1_corrections_cnf": {
    "value": true,
    "units": "flag",
    "description": "Flag that activates the CAL1 corrections: Deactivated (false); Activated (true)"
  },
  "flag_cal1_intraburst_corrections_cnf": {
```



```
"value": true,
"units": "flag",
  "description": "Flag that activates the CAL1 intraburst corrections: Deactivated
(false); Activated (true)"
},
"flag_surface_focusing_cnf": {
  "value": false,
  "units": "flag",
  "description": "Flag that activates the surface focussing: Deactivated (false);
Activated (true)"
},
"surface_focusing_lat_cnf": {
  "value": 0.0,
  "units": "Degrees North",
  "description": "Location of the surface focusing target (latitude) (ignored unless
flag_surface_focusing_cnf is 'true')"
},
"surface_focusing_lon_cnf": {
  "value": 0.0,
  "units": "Degrees East",
  "description": "Location of the surface focusing target (longitude) (ignored unless
flag_surface_focusing_cnf is 'true')"
},
"surface_focusing_alt_cnf": {
  "value": 0.0,
  "units": "m",
  "description": "Location of the surface focusing target (altitude) (ignored unless
flag_surface_focusing_cnf is 'true')"
},
"flag_azimuth_processing_method_cnf": {
  "value": "exact",
  "units": "flag",
  "description": "Flag that indicates the azimuth processing method: Approximate
('approx'); Exact ('exact')"
},
"flag_postphase_azimuth_processing_cnf": {
  "value": false,
  "units": "flag",
  "description": "Flag that enables the post-phase azimuth processing: Deactivated
(false); Activated (true)"
},
"flag_azimuth_windowing_method_cnf": {
  "value": "hamming",
  "units": "flag",
  "description": "Flag the sets the azimuth windowing method: Disabled ('none');
Boxcar ('boxcar'); Hamming ('hamming'); Hanning ('hanning')"
},
"azimuth_window_width_cnf": {
  "value": 64,
  "units": "count",
  "description": "Width of Azimuth window (minimum value: 32, maximum value: 64)"
},
"flag_doppler_range_correction_cnf": {
  "value": true,
  "units": "flag",
  "description": "Flag that activates the Doppler range correction in the geometry
corrections: Deactivated (false); Activated (true)"
},
"flag_slant_range_correction_cnf": {
  "value": true,
  "units": "flag",
  "description": "Flag that activates the slant range correction in the geometry
corrections: Deactivated (false); Activated (true)"
},
"flag_window_delay_alignment_method_cnf": {
  "value": 0,
  "units": "flag",
```




```
"description": "Flag to indicate the window delay alignment method: Surface dependent  
(0); Beam max integrated power (1); Satellite position above surface (2); Look angle 0  
(3); Doppler angle 0 (4)"  
,  
"flag_stack_masking_cnf": {  
  "value": true,  
  "units": "flag",  
  "description": "Flag that activates the Stack Masking algorithm: Activated (true);  
Deactivated (false)"  
},  
"flag_avoid_zeros_in_multilooking_cnf": {  
  "value": true,  
  "units": "flag",  
  "description": "Flag that indicates if the samples set to zero in the beams will be  
avoided when averaging in multi-looking: No (false); Yes (true)"  
},  
"flag_surface_weighting_cnf": {  
  "value": true,  
  "units": "flag",  
  "description": "Flag that activates the surface weighting: Deactivated (false);  
Activated (true)"  
},  
"flag_antenna_weighting_cnf": {  
  "value": false,  
  "units": "flag",  
  "description": "Flag that activates the antenna weighting: Deactivated (false);  
Activated (true)"  
},  
"zp_fact_range_cnf": {  
  "value": 2,  
  "units": null,  
  "description": "Zero padding factor used during range compression"  
},  
"N_looks_stack_cnf": {  
  "value": 240,  
  "units": null,  
  "description": "Number of looks in 1 stack"  
},  
"output_format_flag_cnf": {  
  "value": "extended",  
  "units": "flag",  
  "description": "Flag that specifies output format: the DeDop extended format  
( 'extended' ) or default Sentinel-3 format ( 'sentinel-3' )"  
}  
}
```



8 Annex C. Patch for DeDop-core-1.5.0-Linux-x86_64.sh installer script

Patch necessary to fix installation issue of DeDop Core from file [DeDop-core-1.5.0-Linux-x86_64.sh](#):

```
--- a/DeDop-core-1.5.0-Linux-x86_64.sh 2019-05-15 20:34:32.259156133 +0200
+++ b/DeDop-core-1.5.0-Linux-x86_64.sh 2019-05-15 20:34:32.267156098 +0200
@@ -1,11 +1,11 @@
-#!/bin/bash
+#!/usr/bin/env bash
#
# NAME: DeDop-core
# VER: 1.5.0
# PLAT: linux-64
-# BYTES: 507640026
-# LINES: 1247
-# MD5: b3bc4573aec0692cea1503bclacd9787
+# BYTES: 475824431
+# LINES: 1249
+# MD5: 3896ba1217aa5c37d732755a520f1edf

export OLD_LD_LIBRARY_PATH=$LD_LIBRARY_PATH
unset LD_LIBRARY_PATH
@@ -165,10 +165,10 @@
fi

# verify the size of the installer
-if ! wc -c "$THIS_PATH" | grep 507640026 >/dev/null; then
- printf "ERROR: size of %s should be 507640026 bytes\\n" "$THIS_FILE" >&2
- exit 1
-fi
+#if ! wc -c "$THIS_PATH" | grep 475824431 >/dev/null; then
+# printf "ERROR: size of %s should be 475824431 bytes\\n" "$THIS_FILE" >&2
+# exit 1
+#fi

if [ "$SBATCH" = "0" ] # interactive mode
then
@@ -955,10 +955,10 @@
printf "PREFIX=%s\\n" "$PREFIX"

# verify the MD5 sum of the tarball appended to this header
-MD5=$(tail -n +1247 "$THIS_PATH" | md5sum -)
-if ! echo "$MD5" | grep b3bc4573aec0692cea1503bclacd9787 >/dev/null; then
+MD5=$(tail -n +1249 "$THIS_PATH" | md5sum -)
+if ! echo "$MD5" | grep 3896ba1217aa5c37d732755a520f1edf >/dev/null; then
printf "WARNING: md5sum mismatch of tar archive\\n" >&2
printf "expected: b3bc4573aec0692cea1503bclacd9787\\n" >&2
+ printf "expected: 3896ba1217aa5c37d732755a520f1edf\\n" >&2
printf "got: %s\\n" "$MD5" >&2
fi

@@ -967,4 +967,4 @@
cd "$PREFIX"

-if ! tail -n +1247 "$THIS_PATH" | tar xf -; then
+if ! tail -n +1249 "$THIS_PATH" | tar xf -; then
```